KAZAN FEDERAL UNIVERSITY

ALAKSHIN E.M., DOOGLAV A.V., MAMIN G.V., TAGIROV M.S.

NUCLEAR MAGNETIC RESONANCE IN SOLIDS

Laboratory practical work

KAZAN

2019

UDC 537.635, 537.611.43

Approved by educational-methodological commission of Institute of Physics of Kazan Federal University

Reviewer:

Prof. **Garifullin I.A.** Zavoisky Physical—Technical Institute of Kazan Scientific Center of the Russian Academy of Sciences

Alakshin E.M., Dooglav A.V., Mamin G.V., Tagirov M.S.

Nuclear magnetic resonance in solids: laboratory practical work/ Alakshin E.M., Dooglav A.V., Mamin G.V., Tagirov M.S. − Kazan: Kazan University Publishing House, 2019. − 91 p.

ISBN

The methodological textbook for laboratory work “Nuclear magnetic resonance in solids” for the master course students recounts the basics of the nuclear magnetic resonance theory in diamagnetic insulating crystals and the experimental principles of nuclear magnetic resonance signals detection by continuous wave and pulsed methods, and also a calculation procedure of the nuclear magnetic resonance line shape as obtained in experiment. The textbook gives a short description and operation principle of laboratory NMR setups.

UDC 537.635, 537.611.43

ISBN

Contents

PART 1
CONTINUOUS WAVE NUCLEAR MAGNETIC RESONANCE IN SOLIDS
Introduction

The purpose of the given work is introduction to basics of a nuclear magnetic resonance (NMR) theory in diamagnetic dielectric crystals and with the experimental principles of nuclear magnetic resonance signals detection by continuous wave (CW) methods. This small handbook does not allow to cover with necessary depth even the basic aspects of CW nuclear magnetic resonance. Therefore the handbook can be viewed only as the elementary introduction into NMR, and the consistent and coherent treatment of the theory and experiment can be found in the following monographies:

1. A. Abragam, The principles of nuclear magnetism. Oxford: Clarendon Press, 1961.
2. C.P. Slichter, Principles of magnetic resonance – Springer-Verlag, Berlin, 1980.
3. A. Lösche, Kerninduktion, Deutscher Verlag der Wissenschaften, Berlin, 1957.
4. M. Goldman, Spin Temperature and Nuclear Magnetic Resonance in Solids, Oxford University Press, 1970.

1. Basics of NMR theory in solids

1.1. Motion of free spins.

The concept of “free spins” implies that the magnetic moment of nucleus or atom does not experience interaction with other atoms of substance, and, strictly speaking, is applicable only to very dilute gases. In solids the atoms are bound with each other by forces of electrostatic and magnetic interaction; however the approach of free spins appears useful here for determination of motion behavior of the elementary magnetic moments affected by static and variable magnetic fields.

The nuclear angular momentum **G** is expressed via the dimensionless spin vector **I** and has the form

$$\mathbf{G} = \hbar\mathbf{I},$$

where $\hbar = h/2\pi$ – Planck constant. The value of nuclear spin I is the greatest possible value of component **I** in some direction (for example, set by external magnetic field). The nuclear spin is not identical with spin vector length, but is related with it via the equation $|\mathbf{I}| = \sqrt{I(I+1)}$.

The nuclear magnetic dipole moment $\boldsymbol{\mu}$ is parallel or antiparallel to a vector of angular momentum **G**, therefore we can write

$$\boldsymbol{\mu} = \gamma \mathbf{G} = \gamma \hbar \mathbf{I}.$$

The quantity γ, called the gyromagnetic ratio, is positive if the magnetic moment is parallel to spin moment and is negative otherwise. The nuclear magnetic moments are measured in units of nuclear magneton:

$$\mu_N = 0.505 \cdot 10^{-23} \text{ erg/Gs}$$

(compare with Bohr magneton $\mu_B = 0.927 \cdot 10^{-20}$ erg/Gs).

The magnetic dipole $\boldsymbol{\mu}$ placed in magnetic field **H** is affected by the moment of force $[\boldsymbol{\mu}\mathbf{H}]$. This moment of force causes the change with time of vector of angular momentum **G** so we can write

$$\frac{d\mathbf{G}}{dt} = [\boldsymbol{\mu}\mathbf{H}] \quad \text{или} \quad \frac{d\mathbf{G}}{dt} = \gamma[\mathbf{G}\mathbf{H}]. \tag{1}$$

According to the solution of this equation, the vectors **G** and $\boldsymbol{\mu}$ precess around a field **H** direction with angular velocity $\boldsymbol{\omega}_0 = -\gamma \mathbf{H}$. How would this motion seem to the observer if he/she is in a coordinate system which rotates around an axis coinciding with direction of vector **H (**rotating frame, RF) ? If such coordinate system rotates relative the laboratory coordinate system (laboratory frame, LF) with angular velocity $\boldsymbol{\omega}$, then the derivative $d\mathbf{G}/dt$, calculated in LF, and the analogous derivative $D\mathbf{G}/Dt$ calculated in RF, are related by the equation

$$d\mathbf{G}/dt = D\mathbf{G}/Dt + [\boldsymbol{\omega}\mathbf{G}].$$

Combining this equation with the previous one, we obtain the equation of motion for moment **G** in RF

$$D\mathbf{G}/Dt = \gamma[\mathbf{G}(\mathbf{H} + \boldsymbol{\omega}/\gamma)]. \tag{2}$$

This equation looks like the initial one, but differs from it, more explicitly, that instead of **H** we have now $\mathbf{H}+\boldsymbol{\omega}/\gamma$. Thus the motion of vectors **G** and $\boldsymbol{\mu}$ in a rotating coordinate system is also a precession, but with angular velocity

$$\boldsymbol{\omega}' = -\gamma\mathbf{H}' = -\gamma\left(\mathbf{H}+\boldsymbol{\omega}/\gamma\right) = \boldsymbol{\omega}_0 - \boldsymbol{\omega}. \qquad (3)$$

As one would expect, this apparent precession velocity is equal to a difference between Larmor frequency $\boldsymbol{\omega}_0$ and angular frequency of rotating coordinate system relative the fixed one. In other words, the effective magnetic field is acting in a rotating coordinate system, and is equal to

$$\mathbf{H}' = \mathbf{H}+\boldsymbol{\omega}/\gamma = \mathbf{H}-\mathbf{H}^*, \qquad (4)$$

where $\mathbf{H}^* = -\boldsymbol{\omega}/\gamma$. It is clear that, when $\boldsymbol{\omega} = \boldsymbol{\omega}_0$, the precession disappears and both vectors **G** and $\boldsymbol{\mu}$ become fixed in a rotating coordinate system; this corresponds to effective field $\mathbf{H}' = 0$.

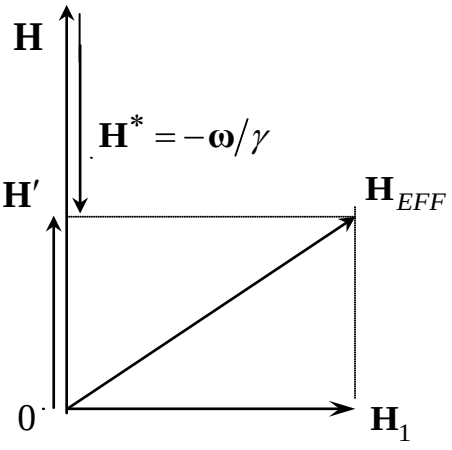

Fig. 1

Using the obtained result it is easy to determine the motion of moments at simultaneous effect of static field **H** for which we suppose to be directed along axis *z* of the Cartesian coordinate system and field $\mathbf{H}_1$ rotating around axis *z* with angular velocity $\boldsymbol{\omega}$ (see Fig. 1). It is obvious that if we go to the coordinate system that is also rotating around axis *z* with angular velocity $\boldsymbol{\omega}$, then that field $\mathbf{H}_1$ will be presented in this system by a constant vector, perpendicular to axis *z*. In this case, the static field **H** must be replaced by the effective field $\mathbf{H}' = \mathbf{H}+\boldsymbol{\omega}/\gamma = \mathbf{H}-\mathbf{H}^*$. Now the equation of motion for moment **G** in a rotating coordinate system becomes

$$D\mathbf{G}/Dt = \gamma\left[\mathbf{G}\left(\mathbf{H}'+\mathbf{H}_1\right)\right] = \gamma\left[\mathbf{G}\,\mathbf{H}_{EFF}\right]. \qquad (5)$$

Here $\mathbf{H}_{EFF}$ – is the vector sum of $\mathbf{H}'$ and $\mathbf{H}_1$. This equation of motion has also the form of initial equation. Hence in a rotating coordinate system the angular

momentum **G** and magnetic moment $\boldsymbol{\mu}$ will experience a precession around a vector $\mathbf{H}_{EFF}$ with angular velocity $-\gamma\mathbf{H}_{EFF}$.

Assume that $\boldsymbol{\omega}=\boldsymbol{\omega}_0$ and that the rotating field $\mathbf{H}_1$ is switched on instantaneously at the time moment $t=0$ when the magnetic moment is along a field $\mathbf{H}$ $\left(\mathbf{H}'=0\right)$. Then the motion of magnetic moment would be a precession around a vector $\mathbf{H}_1$ and at that during each half-period of this motion the direction of $\boldsymbol{\mu}$ would change from parallel to field **H** to antiparallel and vice versa. In a rotating coordinate system this motion occurs in a plane, perpendicular to $\mathbf{H}_1$. Since $H_1 << H$ the frequency of precession around $\mathbf{H}_1$ is much less compared with ω_0; so in a laboratory coordinate system the motion of vector $\boldsymbol{\mu}$ represents a fast rotation around the field **H** with simultaneous slow change of angle $\alpha(=\boldsymbol{\mu}\mathbf{H})$ from 0 to π and back.

If the rotation frequency of $\mathbf{H}_1$ is not equal to Larmor frequency of precession, then the magnetic moment $\boldsymbol{\mu}$ in a rotating coordinate system precesses around the field $\mathbf{H}_{EFF}$. This field makes an angle θ with direction of **H** defined by expression

$$\mathrm{tg}\,\theta = H_1/H' = H_1/\left(H+\omega/\gamma\right). \tag{6}$$

The value of angle α at the time moment *t* (it is supposed that α=0 at *t* = 0) can be found from simple geometrical proportions (see Fig. 2):

$$\sin\frac{\alpha}{2} = \sin\theta\cdot\sin\left(\frac{1}{2}\gamma H_{EFF}t\right), \tag{7}$$

$$\cos\alpha = 1-2\sin^2\theta\cdot\sin^2\left(\frac{1}{2}\gamma H_{EFF}t\right),$$

where $\gamma H_{EFF} = \left[\left(\omega-\omega_0\right)^2+\left(\gamma H_1\right)^2\right]^{1/2}$.

It is clear that the maximum value of α is equal to 2θ and, if $H_1 << H$ (normal case), this value is large only when the value of ω is close enough to ω_0.

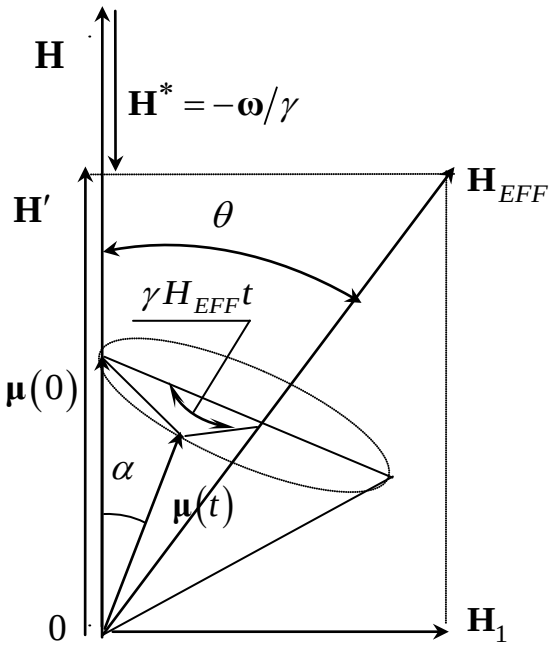

Fig. 2

Thus the effect has resonant character; this possibility to considerably change the orientation of magnetic moment $\boldsymbol{\mu}$ relative a static field **H** by affecting with rather small rotating field H_1 is the phenomenon of magnetic resonance. When $\omega = \omega_0$ the magnetic moment $\boldsymbol{\mu}$ can be turned on 180° by the effect of the rotating field $\mathbf{H}_1$. Ideally it will occur at any value of the field H_1, whatever small it would be, though, of course, the flip velocity is proportional to the value of H_1.

1.2. Magnetic resonance in the systems of coupled spins

1. When dealing with the system of magnetic dipoles fixed in space, it is more convenient to operate with magnetization **M** or magnetic moment of the total system, rather than magnetic moments of individual particles. The magnetic moment of the whole system is simply the vector sum of separate magnetic moments. Therefore the system of spins as a whole will follow the classical equation of motion:

$$d\mathbf{M}/dt = \gamma[\mathbf{MH}]. \tag{8}$$

Our systems of interest are the systems in which the individual dipoles interact weakly with each other, i.e. the dipoles for which the static magnetic susceptibility in the high temperature approach $\mu H/kT << 1$ obeys the Curie law:

$$\chi_0 = N\gamma^2 \hbar^2 I(I+1)/3kT \tag{9}$$

(N – number of particles).

2. We will take into account the peculiarities of magnetic resonance in system of coupled spins by disclaiming the assumption that all changes of orientation and the

value of magnetization are caused entirely by external magnetic fields, and in addition taking into account two main types of internal interactions in condensed matter: 1) interaction of dipoles with thermal oscillations of a lattice and 2) their interaction with each other. Both these interactions are usually much weaker compared with the Zeeman interaction with external fields, but important due to their cumulative effect during the long-term time intervals. The main distinction between them is that only the first interaction (thermal excitations) can change the energy of spin system whereas the second holds this energy invariable.

The main part of spin system energy is the Zeeman energy in a static magnetic field $-(\mathbf{MH}) = -M_z H$. Hence the main changes in energy are due to changes of magnetization component M_z. Suppose that at some time moment the magnetization component M_z is not equal to its equilibrium value $M_0 = \chi_0 H$. We can assume (and this guess appears to be a good approximation for reality) that magnetization recovery occurs with the exponential law according to the differential equation:

$$\dot{M}_z = -(M_z - M_0)/T_1. \qquad (10)$$

Here T_1 – characteristic time constant sometimes called the “longitudinal relaxation time”, since it determines the changes of M_z component, parallel to static magnetic field. More often this constant is called the "spin-lattice relaxation” time as it is related to energy exchange between spin system and lattice in which the dipoles are embedded.

Interaction of two identical dipoles in strong field **H** can be described within the classical point of view as follows. The first dipole $\boldsymbol{\mu}_1$ precesses with the Larmor frequency around field **H** and, hence, possesses a static component along this field and a component which rotates in a plane perpendicular to the field. The static component $\boldsymbol{\mu}_1$ creates in the dipole $\boldsymbol{\mu}_2$ location a weak static field ($\sim \mu_1/r^3$) which orientation relative **H** depends on relative positions of spins. Since **H** is the strong field it is affected considerably only by the component of weak field parallel or antiparallel to it. Each spin in a lattice has a few neighbors with various relative

positions and orientations, therefore the static component of the local field has different values in various places that leads to distribution of Larmor frequencies and a broadening of resonance absorption line. The rotating component $\boldsymbol{\mu}_1$ creates in the location of $\boldsymbol{\mu}_2$ the local magnetic field rotating with Larmor frequency $\boldsymbol{\mu}_1$ which coincides with Larmor frequency for $\boldsymbol{\mu}_2$. In turn it has a component in a plane, perpendicular to **H**, and, hence, can appreciably change orientation of $\boldsymbol{\mu}_2$ due to the resonance phenomenon. The corresponding line width should be of order of a rotating field magnitude. In the considered case it of the same order of magnitude as the local static field and, hence, makes the comparable contribution to the broadening.

3. Here it is necessary to consider the distinction between homogeneous and inhomogeneous broadenings. The line is considered as inhomogeneously broadened if the width is caused by distribution of Larmor frequencies of various magnetic moments in the sample. The origins of this distribution are manifold – from heterogeneity of external magnetic field to the local changes of gyromagnetic ratio γ caused by interaction of dipoles with their environment. Whatever the origin is, the inhomogeneous broadening has one common feature: the phase coherence loss caused by a fan-shaped discrepancy of individual precessing dipoles in *xy* plane is not irreversible. There is a method known as "spin echo" with which help the phase coherence can be recovered.

If the line width as a whole is caused by relaxation effects then the resonance line is considered as "homogeneously broadened". The precessing components of a dipole field induce the so-called "flip-flop" transitions at which one dipole loses the energy, and another gains it. The flip-flop process is most effective when dipoles precess with identical frequency. At this mutual reorientation of the moments the total value of M_z is conserved and the total energy of system remains invariable. The total values of M_x and M_y, on the contrary, are not conserved; as a result of reorientation of spins there is a gradual violation of phase coherence between the components of individual dipoles in *xy* plane, and precessing magnetization in this plane decreases gradually to zero. The flip-flop process sets the "true" time of

transverse or spin-spin relaxation T_2. Following Bloch, we suppose, that the magnetization components M_x and M_y obey the differential equations:

$$\dot{M}_x = -M_x/T_2, \quad \dot{M}_y = -M_y/T_2. \tag{11}$$

4. As before, we assume that spin system is affected by static magnetic field directed along axis *z*, and field $\mathbf{H}_1$ rotating with frequency $\boldsymbol{\omega}$ in *xy* plane and with components $H_{1x} = H_1 \cos\omega t, \quad H_{1y} = H_1 \sin\omega t.$ Equations of motion for the magnetization (8) are as follows:

$$\begin{aligned}
\dot{M}_x &= \gamma\left(M_y H - M_z H_1 \sin\omega t\right), \\
\dot{M}_y &= \gamma\left(-M_x H + M_z H_1 \cos\omega t\right), \\
\dot{M}_z &= \gamma H_1\left(M_x \sin\omega t - M_y \cos\omega t\right).
\end{aligned} \tag{12}$$

With the account of relaxation effects they can be presented in the following form:

$$\begin{aligned}
\dot{M}_x - \gamma H M_y + M_x/T_2 &= -\gamma H_1 M_z \sin\omega t, \\
\dot{M}_y + \gamma H M_x + M_y/T_2 &= \gamma H_1 M_z \cos\omega t, \\
\dot{M}_z + \left(M_z - M_0\right)/T_1 &= \gamma H_1\left(M_x \sin\omega t - M_y \cos\omega t\right).
\end{aligned} \tag{13}$$

For the first time these equations have been given by F. Bloch. It shall be noted that unlike the equation (10), which is valid for any aggregated state of substance, the equations (11) are valid, strictly speaking, only for the magnetic moments at fast motion relative each other, i.e. for fluids and gases. From the equation (11) it follows that the transverse magnetization amplitude decay with time has the exponential law. It can be shown that exponential decay of transverse magnetization $\sim\exp\left(-t/T_2\right)$ corresponds to the Lorentz form of the resonance line:

$$f(\omega) = \frac{1}{\pi}\cdot\frac{T_2}{1+\left(\omega-\omega_0\right)^2 T_2^2} = \frac{1}{\pi}\cdot\frac{\Delta\omega}{\left(\Delta\omega\right)^2+\left(\omega-\omega_0\right)^2} \tag{14}$$

($T_2^{-1} = \Delta\omega$ – line width). However it is known that magnetic resonance lines in solids have the form more often close to the Gaussian form. Below we will obtain the

solutions of equations of motion for magnetization (13) for the case of slow passage through the resonance conditions. Though it is impossible to consider these solutions as adequate description of magnetic resonance in solids they can be used for the qualitative analysis of the phenomenon.

Let's search for the stationary solution corresponding to the forced precession of magnetization around a static magnetic field with angular velocity of the applied field $\mathbf{H}_1$:

$$\begin{aligned} M_x &= M\sin\theta\cdot\cos\omega t, \\ M_y &= M\sin\theta\cdot\sin\omega t, \\ M_z &= M\cos\theta. \end{aligned} \tag{15}$$

Further it is convenient to replace the transverse components M_x and M_y with

$$\begin{aligned} M_+ &= M_x + iM_y = M\sin\theta\cdot\exp(i\omega t), \\ M_- &= M_x - iM_y = M\sin\theta\cdot\exp(-i\omega t). \end{aligned} \tag{16}$$

Suppose that the velocity of passage through the resonance conditions is very small and for all moments of time the stationary requirements do prevail: $M_z = const$ or $\dot{M}_z = 0$. Then Bloch equations have the following form:

$$\begin{aligned} &\dot{M}_+ + i\gamma H M_+ + M_+/T_2 = i\gamma M_z H_1\exp(i\omega t), \\ &\dot{M}_- - i\gamma H M_- + M_-/T_2 = -i\gamma M_z H_1\exp(-i\omega t), \\ &(M_z - M_0)/T_1 = \frac{1}{2}i\gamma\left[M_+\exp(-i\omega t) - M_-\exp(i\omega t)\right]H_1. \end{aligned} \tag{17}$$

Taking into account that

$$\dot{M}_+ = i\omega M_+, \quad \dot{M}_- = -i\omega M_- \text{ (see (16))},$$

from the first two equations (17) we find

$$\begin{aligned} M_+ &= \frac{\gamma H_1 M_z}{\omega + \gamma H - i/T_2}\exp(i\omega t), \\ M_- &= \frac{\gamma H_1 M_z}{\omega + \gamma H - i/T_2}\exp(-i\omega t). \end{aligned} \tag{18}$$

Substituting these solutions into the third Bloch equation (17) we obtain the expression for longitudinal magnetization $\left(\omega_0 = -\gamma H\right)$:

$$M_z = \frac{1+\left(\omega-\omega_0\right)^2 T_2^2}{1+\left(\omega-\omega_0\right)^2 T_2^2 + \gamma^2 H_1^2 T_1 T_2} M_0, \tag{19}$$

from which it is clear that the component M_z is practically always equal to M_0 and even at resonance it differs from M_0 only a little, if $\gamma H_1^2 T_1 T_2 << 1$. The combination of (18) and (19) gives the expression for the component of transverse magnetization:

$$M_{\pm} = \frac{\left[\left(\omega-\omega_0\right)T_2 \pm i\right]\gamma H_1 T_2 \exp\left(\pm i\omega t\right)}{1+\left(\omega-\omega_0\right)^2 T_2^2 + \gamma^2 H_1^2 T_1 T_2} M_0. \tag{20}$$

In general, the solutions (19) and (20) correspond to magnetization vector precession around the field **H** with angle θ to it such that

$$\mathrm{tg}\,\theta = \frac{\left|M_{\pm}\right|}{M_z} = \frac{\gamma H_1 T_2}{\left[1+\left(\omega-\omega_0\right)^2 T_2^2\right]^{1/2}}. \tag{21}$$

In the majority of experiments the passage through the resonance conditions is carried out by change of field H and frequency ω remains constant. Therefore it is convenient to express the value of $\mathrm{tg}\,\theta$ via the magnetic fields. Bearing in mind that $H^* = -\omega/\gamma$ – resonant field for frequency ω and $\Delta H = 1/\gamma T_2$ – resonance line width, we can rewrite (21) in the following form:

$$\mathrm{tg}\,\theta = \frac{H_1}{\left[\left(\Delta H\right)^2 + \left(H - H^*\right)^2\right]^{1/2}}. \tag{22}$$

Usually, when studying magnetic resonance by the stationary method the amplitude of oscillating field is selected much less than the line width; therefore the angle θ is close to zero even at the resonance.

Let's find the behavior of projection of magnetization to a plane, perpendicular to static magnetic field **H** at a resonance. The angle of this projection with a vector of oscillating field $\mathbf{H}_1$ can be found from the expression:

$$\mathrm{tg}\varepsilon = \frac{|M_x|}{|M_y|} = \frac{|M_+ + M_-|}{|M_+ - M_-|}. \qquad (23)$$

Substituting (18) into (23) we obtain:

$$\mathrm{tg}\varepsilon = \left[T_2\left(\omega + \gamma H\right)\right]^{-1} = \frac{\Delta H}{H - H^*}. \qquad (23\ \text{a})$$

Thus, when passing the resonance condition the orientation of vector of transverse magnetization relative the field $\mathbf{H}_1$ changes from parallel to antiparallel; at resonance $\left(H = H^*\right)$ the vector of transverse magnetization makes an angle $\pi/2$. with $\mathbf{H}_1$.

5. The oscillating part of magnetization can be expressed via complex susceptibility:

$$M_+ = \gamma H_1 \exp\left(i\omega t\right). \qquad (24)$$

Using (24) we will write the expressions for the real and imaginary parts of complex susceptibility:

$$\frac{\chi}{\chi_0} = \frac{M_+ / H_1 \exp\left(i\omega t\right)}{M_0 / H} = \frac{\chi'}{\chi_0} - i\frac{\chi''}{\chi_0}. \qquad (25)$$

Substituting (20) in (25) we obtain:

$$\begin{aligned} \frac{\chi'}{\chi_0} &= \frac{\omega_0\left(\omega - \omega_0\right)}{\left(\omega - \omega_0\right)^2 + \left(\Delta\omega\right)^2 + \gamma^2 H_1^2 T_1\left(\Delta\omega\right)}, \\ \frac{\chi''}{\chi_0} &= \frac{\omega_0 \cdot \Delta\omega}{\left(\omega - \omega_0\right)^2 + \left(\Delta\omega\right)^2 + \gamma^2 H_1^2 T_1\left(\Delta\omega\right)} \end{aligned} \qquad (26)$$

(in equations (26) the notation $\Delta\omega = 1/T_2$ is used).

Thus, the real part of susceptibility at resonance is equal to zero and away from a resonance it is either positive (if $\omega_0 > \omega$), or negative (if $\omega_0 < \omega$). The imaginary part of susceptibility at resonance has a maximum and, if $\gamma^2 H_1^2 T_1 << \Delta\omega$,

$$\chi'' / \chi_0 = \omega_0 / \Delta\omega. \qquad (27)$$

This means that imaginary part of complex susceptibility is much larger the static susceptibility if the line width is small compared with resonance frequency.

Therefore the resonance methods are more sensitive in $\omega_0/\Delta\omega$ times compared with the static methods.

6. It was mentioned above that when the requirement $\gamma^2 H_1^2 T_1 T_2 << 1$ is fulfilled the value of longitudinal component of magnetization differs a little from M_0 even at the moment of resonance. At resonance the value

$$M_z = \frac{1}{1+\gamma^2 H_1^2 T_1 T_2} M_0 \tag{28}$$

can be small only as a result of saturation effect of resonance line by the strong radio-frequency field H_1. This occurs because the spin system absorbs energy of oscillating fields with some rate dW/dt and this absorption elevates the spin system temperature until dW/dt is not equal to velocity of energy transfer from spin system to the lattice. Naturally, the temperature of spin system increases with H_1 and is higher the longer are the times of spin-lattice (T_1) and spin-spin (T_2) relaxations.

7. What is the energy of radio-frequency field absorption rate by spin-system? In other words, what is the absorbed power?

We have

$$\overline{\frac{dW}{dt}} = -\overline{M\frac{dH}{dt}} = -\overline{\left(M_x \frac{dH_x}{dt} + M_y \frac{dH_y}{dt}\right)}, \tag{29}$$

where $H_x = H_1 \cos\omega t,\ H_y = H_1 \sin\omega t.$

Substituting the expressions for the transverse magnetization components into (29)

$$\begin{aligned} M_x &= \mathrm{Re}\, M_+ = \mathrm{Re}\, \chi H_1 \exp(i\omega t) = H_1(\chi' \cos\omega t + \chi'' \sin\omega t), \\ M_y &= \mathrm{Im}\, M_+ = H_1(\chi' \cos\omega t - \chi'' \sin\omega t) \end{aligned} \tag{30}$$

and after averaging, we obtain

$$\overline{\frac{dW}{dt}} = \omega H_1^2 \chi''. \tag{31}$$

Thus, the power absorbed at resonance is proportional to the imaginary part of complex susceptibility. For this reason the quantity χ'' is often simply called the absorption.

8. The frequency dependence of $\chi''(\omega)$ sets the line shape of resonance absorption. In the microscopic theory it is shown that generally the imaginary part of complex susceptibility is related to static susceptibility via relation

$$\chi''(\omega) = \pi\omega f(\omega)\chi_0, \tag{32}$$

where $f(\omega)$ – so-called line shape function, satisfying the normalization condition:

$$\int_0^\infty f(\omega)d\omega = 1. \tag{33}$$

With suitable choice of the line shape function $f(\omega)$ the expression (32) is similar to the expression (27) obtained by us from the macroscopic equations. Really, the equation (27) can be easily obtained from the equation (32) substituting the Lorentz shape function into the latter (14).

9. In expression (32), as we see, there are no quantum-mechanical quantities. This is a consequence of the so-called Kramers-Kronig relations which relate the real and imaginary parts of complex susceptibility. The derivation of these relations is given in the monograph [1]. When applied to our problem the Kramers-Kronig relations can be presented the following form:

$$\begin{aligned} \chi'(\omega) &= \frac{1}{\pi}\int_0^\infty \frac{\omega'\chi''(\omega')d\omega'}{\omega'^2 - \omega^2}, \\ \chi''(\omega) &= -\frac{\omega}{\pi}\int_0^\infty \frac{\chi'(\omega')d\omega'}{\omega'^2 - \omega^2}. \end{aligned} \tag{34}$$

From the first relation it follows that the static magnetic susceptibility is equal to:

$$\chi_0 = \chi'(0) = \frac{1}{\pi}\int_0^\infty \frac{\chi''(\omega')}{\omega'}d\omega'. \tag{35}$$

Really, substituting the imaginary part of susceptibility from (32) into (35) we obtain:

$$\frac{1}{\pi}\int_0^\infty \frac{\chi''(\omega)}{\omega}d\omega = \chi_0\int_0^\infty f(\omega)d\omega = \chi_0.$$

Here it is necessary to note that equations (26) for χ' and χ'', obtained by us from the macroscopic equations of motion for magnetization, contain the terms with H_1

and satisfy the Kramers-Kronig relations only in the extreme case of small H_1. At larger amplitudes H_1 there is a saturation, the spin system temperature becomes higher compared with the temperature of crystal lattice, and magnetization is not a linear function of H_1. The Kramers-Kronig relations are valid only for the linear systems.

1.3. Dipole-dipole interactions in the rigid lattice

The broadening of resonance lines is caused by variety of physical reasons. The most simple among them is the inhomogeneity of the applied static magnetic field. In the usual magnets that create magnetic fields of ~10^4 Gs the deviation of magnetic field from the average value is about a few tenth of gauss; with the help of special complex equipment this value can be lowered to a few milligauss. The field homogeneity within the magnetic sample depends on the sample dimensions. The samples with volumes from 0.1 cm^3 to few cubic centimeters are usually used.

For the nuclei having the electric quadrupole moments a few resonance lines can be observed. The occurrence of these lines is related to interaction of the nuclear quadrupole moment with crystal electric field. This leads to considerable broadening of the resonance lines. The equilibrium value of population densities of Zeeman levels of the system is related to transitions between these levels due to effect of spin-lattice interaction. Due to these transitions the system lifetime at any one level will be limited that leads to additional line broadening on $\hbar/T_1$ in energy units.

In this section we will neglect all effects mentioned above and will concentrate our attention to the mechanism of resonance lines broadening related with dipole-dipole interaction between the magnetic moments of various nuclei. In many cases this is allowed. In particular, it is justified when spins of separate nuclei are equal to $1/2$ (in this case the quadrupole moments of nuclei are equal to zero) and the spin-lattice relaxation time is large enough.

It is easy to estimate the order of magnitude of the dipole-dipole interactions contribution to resonance line width. If the distance between the neighboring nuclei with magnetic moments μ is equal to *r*, then each nucleus will create a magnetic field H_{LOK} in the neighboring nucleus position, which order of magnitude is equal to:

$$H_{LOK} = \mu / r^3. \tag{36}$$

If we accept that r = 2 Å and μ =10^{-23} erg/gauss (two nuclear magnetons), then H_{LOK} ; 1 Gs. Since this field can have various orientations relative to the static field $\mathbf{H}_0$, the resonance frequencies of separate nuclei will be distributed within the range of 1 Gs. The resonance energy absorption will be observed within the same range. From these reasoning it follows that the resonance line width does not depend on external magnetic field *H*.

The classical expression for interaction energy of two magnetic moments $\boldsymbol{\mu}_j$ and $\boldsymbol{\mu}_k$ has the following form:

$$E_{jk} = \frac{\boldsymbol{\mu}_j \boldsymbol{\mu}_k}{r_{jk}^3} - 3\frac{\left(\boldsymbol{\mu}_j \mathbf{r}_{jk}\right)\left(\boldsymbol{\mu}_k \mathbf{r}_{jk}\right)}{r_{jk}^5}. \tag{37}$$

To obtain the quantum-mechanical interaction Hamiltonian it is necessary to put in (37) the corresponding operators

$$\boldsymbol{\mu}_j = \gamma_j \hbar \mathbf{I}_j, \quad \boldsymbol{\mu}_k = \gamma_k \hbar \mathbf{I}_k. \tag{38}$$

instead of vectors $\boldsymbol{\mu}_j$ and $\boldsymbol{\mu}_k$. The total Hamiltonian of system comprising *N* identical interacting spins in strong external magnetic field can be written in the form:

$$\mathsf{H} = \mathsf{H}_Z + \mathsf{H}_d, \tag{39}$$

where

$$\mathsf{H}_Z = -\gamma \hbar H \sum_{j=1}^{N} I_{zj} \tag{40}$$

– energy in external magnetic field, and

$$\mathsf{H}_d = \gamma^2 \mathsf{h}^2 \sum_{j<k} \left\{ \frac{\mathbf{I}_j \mathbf{I}_k}{r_{jk}^3} - 3 \frac{\left(\mathbf{I}_j \mathbf{r}_{jk}\right)\left(\mathbf{I}_k \mathbf{r}_{jk}\right)}{r_{jk}^5} \right\} \tag{41}$$

– dipole-dipole interaction energy**.**

Further, to make the equations less cumbersome, where it cannot cause misunderstanding, we will drop the indices *j* and *k* of spherical coordinates *r*, θ, and φ. Then

$$\mathsf{H}_d = \gamma^2 \mathsf{h}^2 \sum \frac{1}{r^3} \left\{ \frac{1}{2}\left(I_+^j I_-^k + I_-^j I_+^k \right) + I_z^j I_z^k - \right.$$

$$\left. -3\left[\frac{\sin\theta}{2}\left(I_+^j e^{-i\varphi} + I_-^j e^{i\varphi} \right) + I_z^j \cos\theta \right] \cdot \left[\frac{\sin\theta}{2}\left(I_+^k e^{-i\varphi} + I_-^k e^{i\varphi} \right) + I_z^k \cos\theta \right] \right\} =$$

$$= \gamma^2 \mathsf{h}^2 \sum \frac{1}{r^3}\left(A_{jk} + B_{jk} + C_{jk} + D_{jk} + E_{jk} + F_{jk} \right), \tag{42}$$

where

$$\begin{aligned}
A_{jk} &= I_z^j I_z^k \left(1 - 3\cos^2\theta\right), \\
B_{jk} &= -\frac{1}{4}\left(1 - 3\cos^2\theta\right)\left(I_+^j I_-^k + I_-^j I_+^k \right) = \frac{1}{2}\left(1 - 3\cos^2\theta\right)\left(I_z^j I_z^k - \mathbf{I}_j \mathbf{I}_k \right), \\
C_{jk} &= -\frac{3}{2}\sin\theta \cdot \cos\theta \cdot e^{-i\varphi}\left(I_z^j I_+^k + I_+^j I_z^k \right), \\
D_{jk} &= C_{jk}^* = -\frac{3}{2}\sin\theta \cdot \cos\theta \cdot e^{i\varphi}\left(I_z^j I_-^k + I_-^j I_z^k \right), \\
E_{jk} &= -\frac{3}{4}\sin^2\theta \cdot e^{-2i\varphi} I_+^j I_+^k, \\
F_{jk} &= E_{jk}^* = -\frac{3}{4}\sin^2\theta \cdot e^{2i\varphi} I_-^j I_-^k.
\end{aligned} \tag{43}$$

Let's consider the interaction of j-th and *k*-th particles. Assume that we choose the representation in which *z* component of spin of each particle is diagonal. Let m_j, m_k, and *M* are the quantum numbers of projections I_z^j, I_z^k, and $I_z^j + I_z^k$. It is easy to show that operators (43) relate the states that differ as follows:

$$
\begin{aligned}
A:&\quad \Delta m_j = 0, \quad \Delta m_k = 0, \quad \Delta M = 0;\\
B:&\quad \Delta m_j = \pm 1, \quad \Delta m_k = \mp 1, \quad \Delta M = 0;\\
C:&\quad \Delta m_j = 0, \quad \Delta m_k = 1, \quad \Delta M = 1;\\
&\qquad\quad 1, \qquad\quad 0, \qquad\quad 0;\\
D:&\quad \Delta m_j = 0, \quad \Delta m_k = -1, \quad \Delta M = -1;\\
&\qquad\quad -1, \qquad\quad 0, \qquad\quad -1;\\
E:&\quad \Delta m_j = 1, \quad \Delta m_k = 1, \quad \Delta M = 2;\\
F:&\quad \Delta m_j = -1, \quad \Delta m_k = -1, \quad \Delta M = -2.
\end{aligned}
$$

We see that matrices *A* and *B* are diagonal in *M* and commute with Zeeman energy matrix (40).

Since the dipole-dipole interaction is much weaker compared to the Zeeman interaction it is natural to try to find out what conclusions can be made about the NMR spectrum and the resonance line shapes on the basis of perturbation theory. Let's consider the energy level $E_M^0 = -\gamma\hbar HM$ corresponding to Hamiltonian (40). This level is strongly degenerate since there are many possible way to combine the separate m_j values and to obtain the value $M = m_1 + m_2 + ... + m_j + ... + m_N$.

The perturbation described by the Hamiltonian H_d splits the level E_M^0 into many sublevels. According to the first perturbation-theory approximation, the first order contribution to level splitting E_M^0 is given only by those terms of the perturbation Hamiltonian which have the matrix elements that differ from zero in the set $|M\rangle$, i.e. only those that acting on a state $|M\rangle$ do not cause change of *M* value. Returning to (44) we see that only operators *A* and *B* satisfy this requirement and should be retained for evaluation of energy correction to E_M^0.

The term *A* has the same form as expression for interaction of two classical dipoles and describes the interaction of one dipole with the static local field created by the other dipole.

The term *B* describes the interaction at which simultaneous flip of the two nearest spins in opposite directions is possible. This part of the Hamiltonian corresponds to resonant effect of the rotating local field.

The effect of term *C* is the admixture of small part of a state $|M-1\rangle$ to a state $|M\rangle$ with unperturbed energy E_M^0. Thus, the exact eigenstate of the Hamiltonian H will be presented in the form $|M\rangle+\alpha|M-1\rangle+...$, where $\alpha-$ small values of the order of H_{LOK}/H.

When affected by variable magnetic field there will be the transitions between two Zeeman levels E_M^0 and $E_{M'}^0$ with the probability, proportional to:

$$\sum_{m_1,...,m_N;m_1',...,m_N'} \left|\left\langle M; m_1, m_2,..., m_j,..., m_N \left| I_x \right| M'; m_1', m_2',..., m_j',..., m_N' \right\rangle\right|^2, \quad (45)$$

where $I_x = \sum_{j=1}^{N} I_x^j$.

From the structure of matrix I_x^j it is clear that $m_j' = m_j \pm 1$, $M' = M \pm 1$; the transitions are possible only between the neighboring Zeeman levels that give one resonance line with frequency ω_0.

This conclusion fails if we go to the next approximation of a perturbation theory. Really, with the account of operators *C*, *D*, *E* and *F* it is possible to present the correct wave functions in the following form:

$$|M\rangle^{(1)} = |M\rangle + \alpha_1|M+1\rangle + \alpha_{-1}|M-1\rangle + \alpha_2|M+2\rangle + \alpha_{-2}|M-2\rangle, \quad (46)$$

where $\alpha_i \sim H_{LOK}/H$. Now the transitions $\Delta M = 0, \pm 2, \pm 3$ with frequencies $0,\ 2\omega_0,\ 3\omega_0$ are possible; the intensity of additional absorption peaks is proportional to α^2.

The matrix *A* + *B* is such that its structure would not change if we reverse the sign of the diagonal elements. Therefore the solution of the secular equation *A* + *B* - *E* = 0 gives for perturbation energy *E* the values which are in pairs identical

by the module, but differ in sign. It is easy to understand that transition probabilities between the two pairs of sublevels, different in energy signs only, will be identical also. It follows that the shape of the main NMR line is symmetric relative the resonance frequency.

The detailed calculations by a perturbation technique are impossible because of large number of degrees of freedom in the system of magnetic particles. Therefore the moments method has a wide application, thus allowing to consider the magnetic dipole interactions and to estimate the resonance line shape without the energy spectrum evaluations. The analysis of magnetic resonance line shape by the method of moments has been performed for the first time by Van Vleck.

1.4. Method of moments and the NMR line shape

The line moments are the important characteristics of the line shapes. The *K* th moment M_K relative the frequency ν_0 is determined by the following equation:

$$M_K = \int_0^\infty (\nu - \nu_0)^K f(\nu) d\nu, \tag{47}$$

where $f(\nu)$ – line shape function.

Let's set $\nu - \nu_0 = u$, $f(\nu) \equiv f(\nu_0 + u) \equiv \overline{f}(u)$;

then $M_K = \int_{-\nu_0}^\infty u^K \overline{f}(u) du$ or for narrow lines:

$$M_K = \int_{-\infty}^\infty u^K \overline{f}(u) du. \tag{48}$$

Let's expand $\overline{f}(u)$ in Fourier integrals:

$$\overline{f}(u) = \frac{1}{2\pi} \int_{-\infty}^\infty \varphi(t) e^{-iut} dt, \quad \varphi(t) = \int_{-\infty}^\infty \overline{f}(u) e^{iut} du. \tag{49}$$

The Fourier transform $\varphi(t)$ of the line shape function has a simple physical meaning. Let the nuclear paramagnet to be in equilibrium state in static magnetic field **H**, so its

magnetization is along this field. If we apply a short intensive pulse of a radio-frequency field so that $\mathbf{H}_1 \perp \mathbf{H}$ to the sample, after its effect the magnetization $\mathbf{M}$ will turn on some angle α relative the field H. Assume that the pulse duration is so small that it is possible to neglect the relaxation phenomena. If the resonance line is infinitely narrow then after the pulse termination the magnetization **M** will precess with frequency $\nu_0 = \omega_0 / 2\pi$ around the field with a constant angle α.

This free precession can be detected from the signal induced by it in the coil, surrounding the sample. If the line width is finite, then due to distribution of precession frequencies the signal will decay during the time of the order of inverse line width. It appears that the Fourier transform of the line shape function is simply related to the free precession decay curve: the function $\varphi(t)$ is proportional to signal amplitude of the free precession upon termination of 90^0 pulse.

Let's expand the function $\varphi(t)$ in Taylor series near the point $t = 0$:

$$\varphi(t) = \varphi(0) + t \left.\frac{d\varphi(t)}{dt}\right|_{t=0} + \frac{t^2}{2!} \cdot \left.\frac{d^2\varphi(t)}{dt^2}\right|_{t=0} + \ldots \qquad (50)$$

From (49) it follows that

$$\left.\frac{d^K\varphi(t)}{dt^K}\right|_{t=0} = i^K M_K, \qquad (51)$$

and if all moments M_K are known, then the shape function $f(\nu)$ can be reconstructed. There are the methods that allow calculations of the moments M_K with high accuracy, however with growing *K* the evaluation becomes so cumbersome that it is necessary to be restricted to calculation of a few first moments only. Therefore for comparison of the theory with experiment one uses several typical curves of which one chooses the closest to a line obtained from experiment. Then it is necessary to compare the known moments of typical curve with the moments obtained theoretically.

The Gaussian and Lorentz functions as the essentially different functions are usually used as the typical curves.

The Gaussian line

$$\overline{f}_G(u) = \frac{1}{\sqrt{2\pi}\sigma} \cdot \exp\left(-u^2/2\sigma^2\right) \tag{52}$$

has mildly sloping peak and the slope goes down rapidly compared with the Lorentz line:

$$\overline{f_L}(u) = \frac{\Delta}{2\pi} \cdot \frac{1}{u^2 + \Delta^2/4}. \tag{53}$$

The line width, determined by equality:

$$\overline{f}(\Delta\nu/2) = \frac{1}{2}\overline{f}(0), \tag{54}$$

for the Gaussian form is equal to:

$$(\Delta\nu)_G = 2\sigma\sqrt{2\ln 2} = 2.35\sigma,$$

and for the Lorentz form it is: $(\Delta\nu)_L = \Delta.$

For the Gaussian line the even moments are equal to:

$$M_2 = \sigma^2,\ M_4 = 3\sigma^4,...,\ M_{2n} = 1\cdot 3\cdot 5\cdots(2n-1)\sigma^{2n}. \tag{55}$$

For the Lorentz line the integrals (48) at $K > 1$ diverge. Therefore, the Lorentz line is cut at frequencies $\nu_0 \pm \alpha,$ where $\alpha >> \Delta/2.$

Then

$$M_2 = \frac{\alpha\Delta}{\pi},\ M_4 = \frac{\alpha^3\Delta}{3\pi},...,\ M_{2n} = \frac{\Delta}{\pi}\cdot\frac{\alpha^{2n-1}}{2n-1}. \tag{56}$$

The Gaussian and Lorentz lines are symmetric in ν_0; therefore the odd moments are equal to zero. To clarify the question how close is the given shape function to the Gaussian or Lorentz line one often limits oneself to evaluations of the relation M_4/M_2^2. For the Gaussian line

$$M_4/M_2^2 = 3, \tag{57}$$

for the Lorentz line

$$M_4/M_2^2 = \alpha\,\pi/3\Delta\ >> 1, \tag{58}$$

for the squared shape line $M_4/M_2^2 = 1.$

1.5. Evaluation of the moments

Let's return to the line width and the line shape broadened due to dipole-dipole interaction. The second moment of the dipolar broadened line is the most simple and interesting, and according to (47) can be determined as

$$M_2 = \left\langle \left(\nu - \nu_0\right)^2 \right\rangle. \tag{59}$$

Because of line symmetry the average frequency $\langle \nu \rangle$ is equal to resonance frequency ν_0 and hence

$$M_2 = \left\langle \nu^2 \right\rangle - \nu_0^2. \tag{60}$$

Let E_n be the eigenvalues of the Hamiltonian H (39). Since the transition between the levels n and n' is characterized by the frequency

$$\nu_{nn'} = \frac{\mathsf{E}_n - \mathsf{E}_{n'}}{h}$$

and the intensity, proportional to $\left|\langle n | I_x | n' \rangle\right|^2$, then

$$\left\langle \nu^2 \right\rangle = \frac{\sum\limits_{n,n'} \nu_{nn'}^2 \left|\langle n | I_x | n' \rangle\right|^2}{\sum\limits_{n,n'} \left|\langle n | I_x | n' \rangle\right|^2}. \tag{61}$$

It is easy to show that this equation can be transformed into the form:

$$\left\langle \nu^2 \right\rangle = -\frac{Sp\left[\mathsf{H}\, I_x\right]^2}{h^2 Sp I_x^2}. \tag{62}$$

Really,

$$Sp\left(\mathsf{H}\, I_x - I_x \mathsf{H}\right)^2 = \sum_{n,n'} \left\langle n \left| \mathsf{H}\, I_x - I_x \mathsf{H} \right| n' \right\rangle \left\langle n' \left| \mathsf{H}\, I_x - I_x \mathsf{H} \right| n \right\rangle.$$

Since the trace (spur) of matrix is invariant relative the similarity transformation, we can assume that the matrix H is diagonal, and then

$$\left\langle n \left| \mathsf{H}\, I_x - I_x \mathsf{H} \right| n' \right\rangle = h\nu_{nn'} \left\langle n | I_x | n' \right\rangle,$$

$$\langle n'|\mathsf{H}\, I_x - I_x \mathsf{H}\,|n\rangle = -h\nu_{nn'}\langle n'|I_x|n\rangle$$

and, therefore

$$Sp\left(\mathsf{H}\, I_x - I_x \mathsf{H}\right)^2 = -h^2 \sum_{n,\,n'} \nu_{nn'}^2 \left|\langle n|I_x|n'\rangle\right|^2.$$

The denominator of the equation (62) is transformed as follows:

$$SpI_x^2 = \sum_{n,n'} \langle n|I_x|n'\rangle\langle n'|I_x|n\rangle = \sum_{n,n'} \left|\langle n|I_x|n'\rangle\right|^2.$$

The validity of the equation (62) is proven. This equation, unlike (61), is very convenient for calculations since the traces of matrices can be easily calculated while the evaluation of eigenvalues of matrices at large N is related to big difficulties.

It is very important to bear in mind the following. In the equation (62) the absorption is considered at all frequencies ν from 0 to ∞. It was pointed above that there are additional absorption peaks at frequencies $0, 2\nu_0, 3\nu_0$ besides the main resonance line at frequency ν_0; though these peaks are weak (they are far from the main line center), their contribution to the higher order moments is very large.

Therefore, since we are only interested in the main resonance line, the Hamiltonian $\mathsf{H} = \mathsf{H}_Z + \mathsf{H}_d$ in the equation (62) shall be replaced by the truncated Hamiltonian $\mathsf{H}_Z + \mathsf{H}_d^0$, neglecting the part of dipole-dipole interaction operator H_d that does not commute with H_Z and, consequently, leads to occurrence of additional resonance absorption peaks. From (44) it follows that

$$\mathsf{H}_d^0 = \sum_{j<k} \frac{\gamma^2 \mathsf{h}^2}{r^3}\left(A_{jk} + B_{jk}\right) = \sum_{j<k} \frac{3}{2}\cdot\frac{\gamma^2\mathsf{h}^2}{r_{jk}^3}\left(1 - 3\cos^2\theta_{jk}\right)\left[I_z^j I_z^k - \frac{1}{3}\left(\mathbf{I}^j\,\mathbf{I}^k\right)\right]. \qquad (63)$$

The detailed calculations of the moments are reduced to evaluations of traces of products of spin matrices

$$\left(I_\alpha^j\right)^{n_1}\left(I_\beta^k\right)^{n_2}\cdots\left(I_\gamma^l\right)^{n_m},$$

where $\alpha, \beta, \gamma = x, y, z;\ j \neq k \neq \ldots \neq l.$ It is useful to note that

$$Sp\left[\left(I_\alpha^j\right)^{n_1}\left(I_\beta^k\right)^{n_2}\ldots\left(I_\gamma^l\right)^{n_m}\right] = 0, \qquad (64)$$

if at least one of the powers n_i is the odd number.

Using (64) it is easy to show that in (62) the cross terms that contain products $\mathsf{H}_Z\mathsf{H}_d^0$ disappear, so (62) transforms into the following equation:

$$\left\langle \nu^2 \right\rangle = -\frac{Sp\left[\mathsf{H}_Z, I_x\right]^2 + Sp\left[\mathsf{H}_d^0, I_x\right]^2}{h^2 SpI_x^2}. \tag{65}$$

If there would be no dipole-dipole interactions and $\mathsf{H}_d^0 = 0$ then it is obvious that $\left\langle \nu^2 \right\rangle = \nu_0^2$. From (60) and (65) we obtain finally:

$$M_2 = -\frac{Sp\left[\mathsf{H}_d^0, I_x\right]^2}{h^2 SpI_x^2}. \tag{66}$$

Similarly, for the fourth moment we have

$$M_4 = \frac{Sp\left[\mathsf{H}_d^0, \left[\mathsf{H}_d^0, I_x\right]\right]^2}{h^4 SpI_x^2}. \tag{67}$$

Evaluations (66) with the Hamiltonian (63) give the following expression for the second moment (Van-Fleck equation):

$$M_2 = \frac{3}{16\pi^2}\gamma^4 \mathsf{h}^2 I\left(I+1\right)\sum_k \frac{\left(1-3\cos^2\theta_{jk}\right)^2}{r_{jk}^6} \text{ [Hz}^2\text{]}. \tag{68}$$

For the powder that contains crystals with chaotic orientations this expression becomes simpler due to <u>disappearance</u> of angular dependence. By averaging over the sphere we obtain $\left(1-3\cos^2\theta\right)^2 = 4/5$ and, hence,

$$M_2 = \frac{3}{4}\gamma^4 \mathsf{h}^2 I\left(I+1\right)\sum_k \frac{\left(1-3\cos^2\theta_{jk}\right)^2}{r_{jk}^6} \text{ [(rad/s)}^2\text{]},$$

$$M_2 = \frac{3}{20\pi^2}\gamma^4 \mathsf{h}^2 I\left(I+1\right)\sum_k r_{jk}^{-6}. \tag{69}$$

For a simple cubic lattice with constant a_0 we have:

$$\sum_k r_{jk}^{-6} = 8.5 a_0^{-6}$$

and

$$M_2 = 5.1 \frac{\gamma^4 \mathsf{h}^2}{4\pi^2} I(I+1) a_0^{-6}. \qquad (70)$$

In the case of single crystal with a simple cubic lattice

$$M_2 = 12.3 \frac{\gamma^4 \mathsf{h}^2}{4\pi^2} I(I+1) a_0^{-6} \left(\lambda_1^4 + \lambda_2^4 + \lambda_3^4 - 0.187 \right) \text{ [Hz}^2\text{]}, \qquad (71)$$

where $\lambda_1, \lambda_2, \lambda_3$ – direction cosines of external field relative the crystal axes; $a_0 = a/2,$ where a – lattice constant.

We note that with the account of only a static part of dipole-dipole interaction

$$\gamma^2 \mathsf{h}^2 \sum_{j<k} A_{jk} r_{jk}^{-3}$$

in the Hamiltonian, the second moment M_2 is $9/4 = (3/2)^2$ times smaller. If, on the contrary, we include all operators from *A* to *F* (see (43)) in our consideration, we will obtain the overestimated value. Simple calculation for a powder shows that replacement H_d^0 with the total Hamiltonian H_d leads to M_2 increase in $10/3$ times.

Knowing only M_2 it is impossible to make conclusions about the resonance line shape. Therefore, using expression (67) it is reasonable to calculate also, at least, the fourth moment. It is possible to present the result of this cumbersome evaluation in the following form:

$$M_4 = \frac{1}{(2\pi)^4} \gamma^8 \mathsf{h}^4 \left\{ 3 \left(\sum_k b_{jk}^2 \right)^2 - \frac{1}{3N} \sum_{jkl\neq} b_{jk}^2 \left(b_{jl} - b_{kl} \right)^2 - \right.$$

$$\left. - \frac{1}{5} \sum_k b_{jk}^4 \left(8 + \frac{3}{2I(I+1)} \right) \right\} \left[\frac{I(I+1)}{3} \right]^2, \qquad (72)$$

where

$$b_{jk} = \frac{3}{2} \cdot \frac{1 - 3\cos^2 \theta_{jk}}{r_{jk}^3},$$

and the symbol $\sum_{jkl\neq}$ means that there should be no two identical indices in threefold summation. The numerical estimate (72) is difficult even for a simple cubic lattice if the magnetic field direction relative the crystallographic axis is arbitrary. If we retain only the first term in curly brackets, then $M_4 = 3\left(M_2\right)^2$, that corresponds to the Gaussian line shape.

2. Continuous wave methods of NMR signal detection

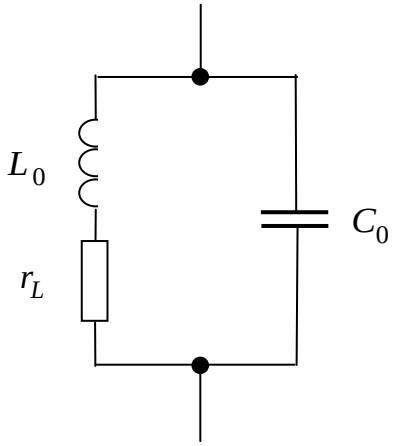

Fig. 3

The experimental aspects of NMR are given in detail in the monography [3]. We will concentrate here only on principles and possibilities of various methods of NMR detection. In the majority of methods the detection of NMR signals is based on registration of changes of LC circuit characteristics into which inductance coil the explored sample is placed. The ohmic losses in the coil of parallel circuit L_0C_0 (Fig. 3) can be taken into account by the series connected resistance r_L. These losses at frequency ω are characterized by a tangent of angle of losses $\mathrm{tg}\delta_L$ and a Q-factor Q:

$$\mathrm{tg}\delta_L = \frac{r_L}{\omega L_0} = \frac{1}{Q};$$

For good coils $Q \sim 100$. The series connected resistance r_L is equivalent to in-parallel connected resistance R_L, related to r_L via the relation

$$\frac{R_L}{\omega L_0} = \frac{\omega L_0}{r_L} = Q.$$

The losses in the capacitor can be also considered by means of in-parallel connected resistance R_C. However, in NMR experiments usually the circuits which Q-factor of capacitors are considerably larger than the Q-factor of coils are used; therefore the losses in capacitors can be neglected (R_C) ≈ ∞.

If we place the sample into the coil its inductance becomes equal to:

$$L = L_0(1 + 4\pi\xi\chi),$$

where $\xi \leq 1$ – coil filling factor determined as the sample volume to working volume ratio of the coil, and $\chi = \chi' - i\chi''$ – complex nuclear magnetic susceptibility, which, as it has been shown in the previous chapter, considerably changes in the vicinity of resonance frequency ω_0.

2.1. Q- meter method

The block scheme of the installation is given in Fig. 4. The conductivity of a parallel circuit is equal to:

$$G = \frac{1}{R} + i\left[\omega C_0 - \frac{1}{\omega L_0(1 + 4\pi\xi\chi)}\right].$$

Since $|4\pi\xi\chi| << 1$ at resonance $\left(\omega C_0 = \frac{1}{\omega L_0}\right)$ we have:

$$G = \frac{1}{R} + i\frac{4\pi\xi\chi}{\omega L_0}.$$

The conductivity changes at magnetic resonance causes the maximum change of high frequency voltage in a circuit in the case when the circuit total current does not vary in magnitude. This requirement is fulfilled, if RF generator has large internal resistance or if the generator is connected with a circuit through the impedance Z_G, which is very large in comparison with the impedance of a parallel circuit, i.e.

$|Z_G| >> |G^{-1}|$ (for example the role of Z_G can be played by large ohmic resistance or small capacitor). The RF voltage loss on circuit is equal to:

$$U = IG^{-1} = IR\frac{1}{1+i4\pi\xi\chi\left(R/\omega L_0\right)} = IR\frac{1}{1+i4\pi\xi\chi Q}$$

and in the absence of NMR signal $(\chi = 0)$

$$U_0 = IR.$$

Since $|4\pi\xi\chi\mathrm{Q}| << 1$, we can write

$$U = U_0\left(1 - i4\pi\xi\chi Q\right) = U_0 + U_\chi,$$

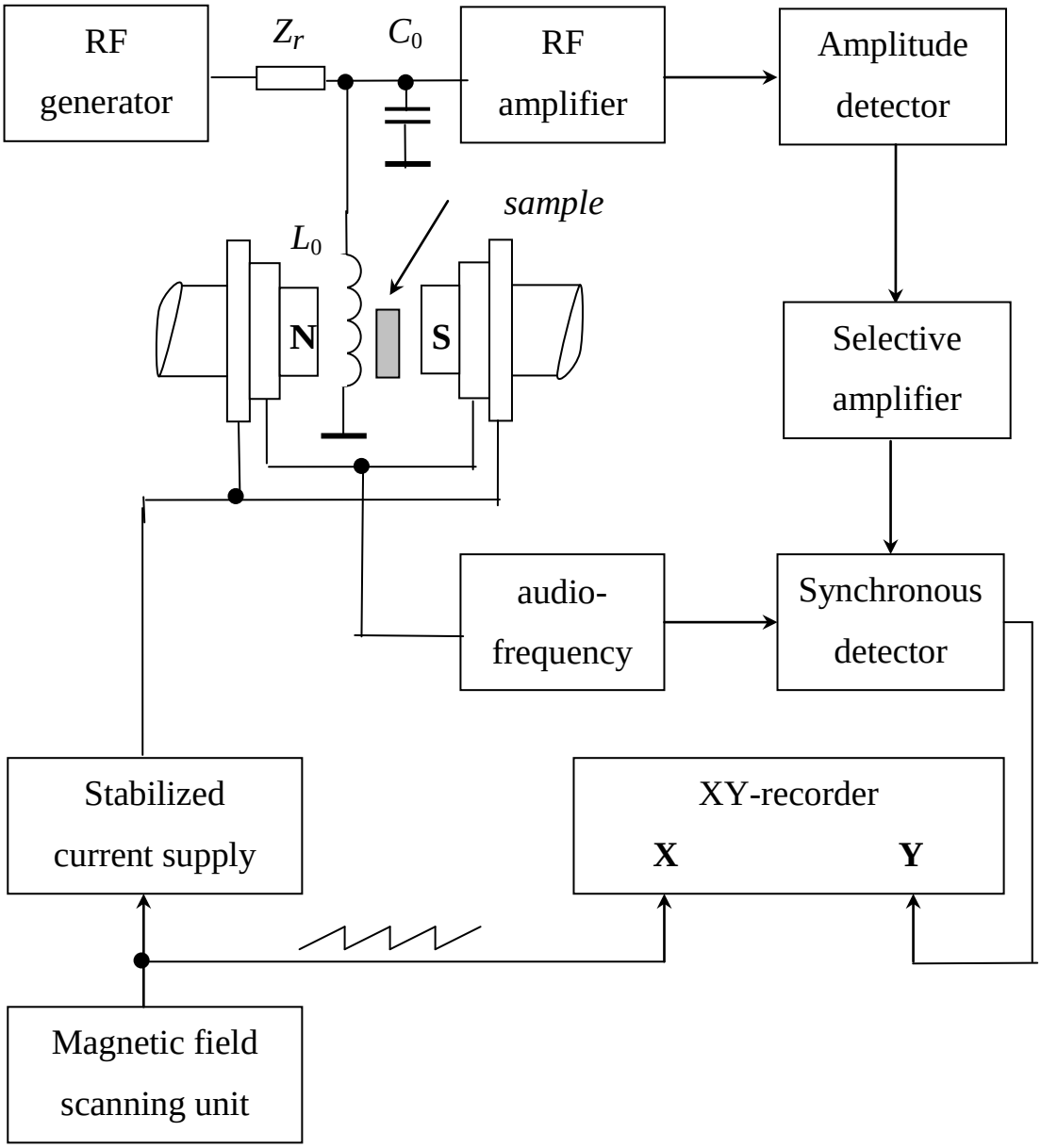

Fig. 4

where $U_\chi = -iU_0 4\pi\xi Q(\chi' - i\chi'') = U_{\chi''} + iU_{\chi'}$; as a result the voltage change on a circuit at a resonance

$$\Delta U = U - U_0 \approx U_{\chi''} = -U_0 \cdot 4\pi\xi\chi'' Q$$

is proportional to imaginary part of complex susceptibility, i.e. absorption. In the Q-meter method the NMR signal appears in the form of very small modulation of the voltage U_0 existing also in the absence of the signal.

2.2. Bridge detector

In the bridge detection method the circuit voltage U_0 is compensated, summing with it, prior to amplification, the voltage U_1, almost equal to it in amplitude and almost opposite in phase. In this case the amplified and detected voltage is equal to:

$$V = U_0 - U_1 - iU_0 \cdot 4\pi\xi\chi Q.$$

For stable operation of the device (block diagram of RF part is shown in Fig. 5) it is desirable to avoid the total compensation and to hold the requirement $|U_0 - U_1| >> \Delta U$. The difference $(U_0 - U_1)$ can have any phase φ relative to U_0. Writing $U_0 - U_1 = \alpha U_0 \exp(i\varphi)$, where α – real quantity, we find:

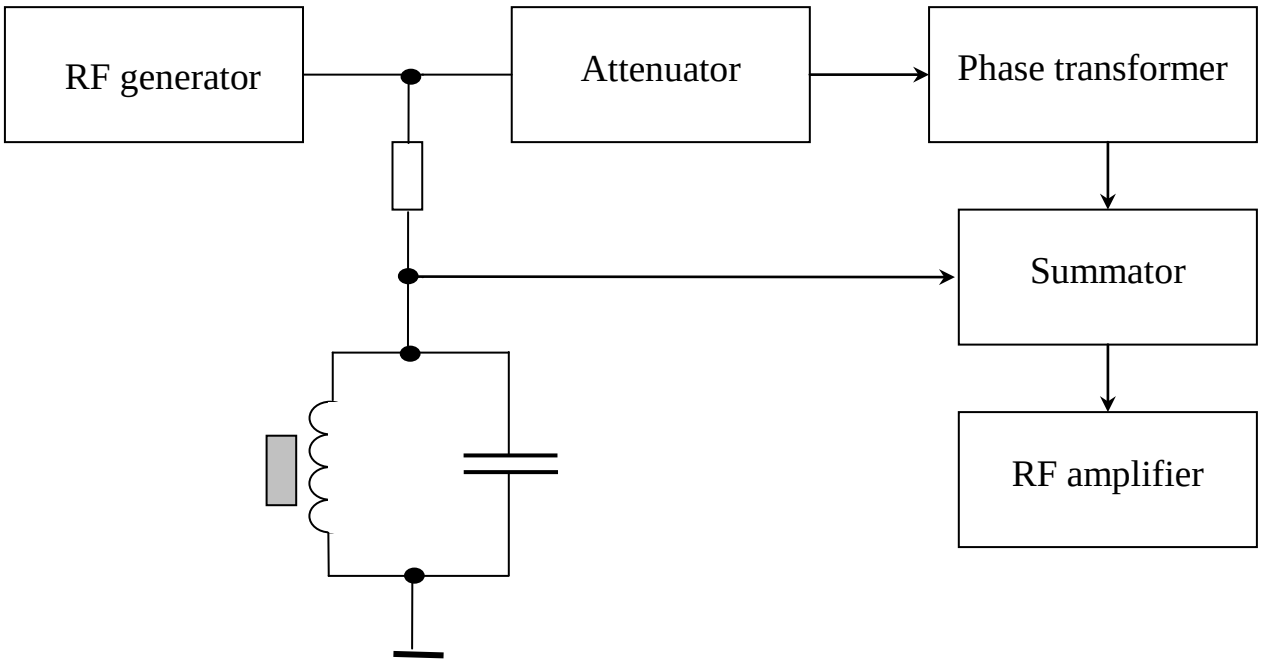

Fig. 5

$$V = \alpha U_0 \exp(i\varphi)\left\{1 - i\frac{4\pi\xi\chi Q}{\alpha}\exp(-i\varphi)\right\} =$$

$$= \alpha U_0 \exp(i\varphi)\left\{1 - \frac{4\pi\xi Q}{\alpha}(\chi'\sin\varphi + \chi''\cos\varphi) - i\frac{4\pi\xi Q}{\alpha}(\chi'\cos\varphi - \chi''\sin\varphi)\right\}.$$

Due to smallness of $4\pi\xi\chi Q/\alpha$ only the first two terms are essential in the curly brackets. At $\varphi = 0$ the amplitude V in the first approximation depends only on χ'' (absorption signal), and at – $\varphi = \frac{\pi}{2}$ only on χ' (dispersion signal). At the intermediate values of φ the incoming voltage from the bridge output on the high-frequency amplifier contains a mixture of absorption and dispersion signals.

2.3. Bloch method (Crossed-coil method)

This system is similar in construction and operation to a bridge in which, however, the functions of creating and recording the high-frequency field are carried out by different coils. The field created by the transmitting coil equalizes the phases of the separate precessing nuclear moments; the receiver coil serves for measuring of the variable magnetic flux appearing as a result of precession of the net magnetization vector.

If the axis of the transmitting coil coincides with axis x of laboratory coordinate system, then the voltage ΔU induced by precessing magnetization in the receiver coil will be proportional to dM_y/dt. Since $M_y = \mathrm{Im}\left(\chi H_1 \exp\left(i\omega t\right)\right)$ (see 30)), then

$$\frac{dM_y}{dt} = H_1 \frac{d}{dt}\left(\chi' \sin\omega t - \chi'' \cos\omega t\right) = H_1\omega\left(\chi' \cos\omega t + \chi'' \sin\omega t\right).$$

The amplitude of this voltage is proportional to $\left(\chi'^2 + \chi''^2\right)^{1/2}$.

If fields of coils are not strictly perpendicular, then the transmitting coil induces a voltage in the receiver coil:

$$V \sim \frac{d}{dt}\left(H_1 \cos\omega t\right) \sim \omega \sin\omega t,$$

that is summed with ΔU. If $|V| >> |\Delta U|$, then the voltage amplitude change on the receiver coil at resonance is equal to

$$|V + \Delta U| - |V| \sim \omega\chi''.$$

Thus, existence of leakage flux when using the crossed coils allows to observe not $\left(\chi'^2+\chi''^2\right)^{1/2}$, but χ'' – pure absorption signal. From the last equation it follows that the voltage amplitude change at resonance has a sign which is determined by sign of $\omega\left(=-\gamma H\right)$ or gyromagnetic ratio sign γ; as a result it is possible to find the relative signs of two nuclear moments $\gamma\hbar I$ and $\gamma'\hbar I'$, by comparing their signals at one frequency, but in different magnetic fields.

2.4. Autodyne detector (generator of weak oscillations)

The operation principle of autodyne detector is as follows. The sample with nuclear spins is located in the coil of LC circuit of the radio-frequency generator. The susceptibility change in the area of resonance causes the frequency and amplitude modulation of the generated high-frequency oscillations. Depending on whether the subsequent receiver reacts on the changes of frequency or amplitude, after detection the dispersion or absorption signal is obtained. In practice the autodyne detectors are used, as a rule, for recording of absorption signals.

It is known that the parallel resonance circuit can be excited by connecting a negative conductance in parallel to it, i.e. a two-terminal network with a volt-ampere characteristic of the type:

$$i = G_1 u + G_2 u^2 + G_3 u^3 + \ldots$$

The oscillations in a circuit arise only in case when the conductivity G_1 in the working point is negative (N-type volt-ampere characteristic). We call the working point the intersection point of the characteristics with axis $u = 0$. Without loss of generality it is possible to consider an inflexion point of a curve as the working point $i = i(u)$, i.e. to set $G_2 = 0$. The stationary oscillations in a circuit with conductivity G will be established under the requirement $G_1 + G = G_1' < 0$. The amplitude of excited oscillations can be found from the graph, by determining the extreme points of the resultant volt-ampere characteristic from the requirement $di/du = 0$:

$$i = G_1' u + G_3 u^3.$$

The position of these points is determined from the expression

$$\pm u_1 = \pm \sqrt{\frac{G_1'}{3G_3}},$$

whence the oscillation amplitude is

$$V_0 = 2u_1 = \sqrt{\frac{4G_1'}{3G_3}}.$$

The sensitivity E of the autodyne detector is characterized by voltage change in the oscillating circuit at change of its conductivity:

$$\mathrm{E} = \frac{dV_0}{dG} = \frac{dV_0}{dG_1'} = \frac{2}{3G_3} \cdot \frac{1}{V_0}.$$

Thus, the sensitivity increases at contraction of oscillation amplitude.

The advantages of autodyne detectors are their simplicity and ease of resetting in a wide frequency band. Their basic deficiency – difficulty to obtain very weak radio-frequency fields H_1, which are sometimes necessary to avoid the NMR signal saturation effect in the samples with long relaxation times.

2.5. Double modulation

Strong NMR signals (for example, from water protons) can be observed on the oscilloscope screen using one low-frequency modulation of magnetic field. Such scheme of observation is realized, for example, in magnetic inductometers ІІІ1–1 and ІІІ1–9. The noise power in this scheme, proportional to transmission bandwidth ΔF of a low-frequency amplifier, is rather high. For example, for observation of undistorted NMR lines at modulation frequency of 50 Hz the transmission bandwidth of low-frequency amplifier should be of the order of 10^3 Hz. For observation of weak signals it is necessary to reduce the noise power, i.e. to reduce the transmission band of low-frequency amplifier; in case of very weak signals the transmission bandwidth

should be less than 0.1 Hz. It is very difficult to create low-frequency amplifiers with such narrow transmission band and to stabilize the modulation frequency within a small part of this band. Therefore we will do the following. Together with slow change of magnetic field with the linear law (modulation 1) we will carry out fast and shallow (much less than NMR line width) modulation with frequency Ω (modulation 2). The resulting change of magnetic field is:

$$H = at + H_M \sin \Omega t$$

($a = const$, $H_M \left(< \Delta H/2\right)-$ modulation depth) leads to that the NMR signal is transferred on fixed frequency Ω, and its amplitude appears to be proportional to derivative of absorption $d\chi''/dH$, and phases of frequency oscillation Ω on different sides of a curve $\chi''(H)$ differ on 180^0 (Fig. 6). The subsequent NMR signal amplification is carried out by the special selective amplifier attuned on modulation frequency Ω and having a transmission band $\Delta F = \Delta\Omega/2\pi$ of the order of several Hz. The selective amplifier is usually constructed as the negative feedback amplifier through the band-rejection filter.

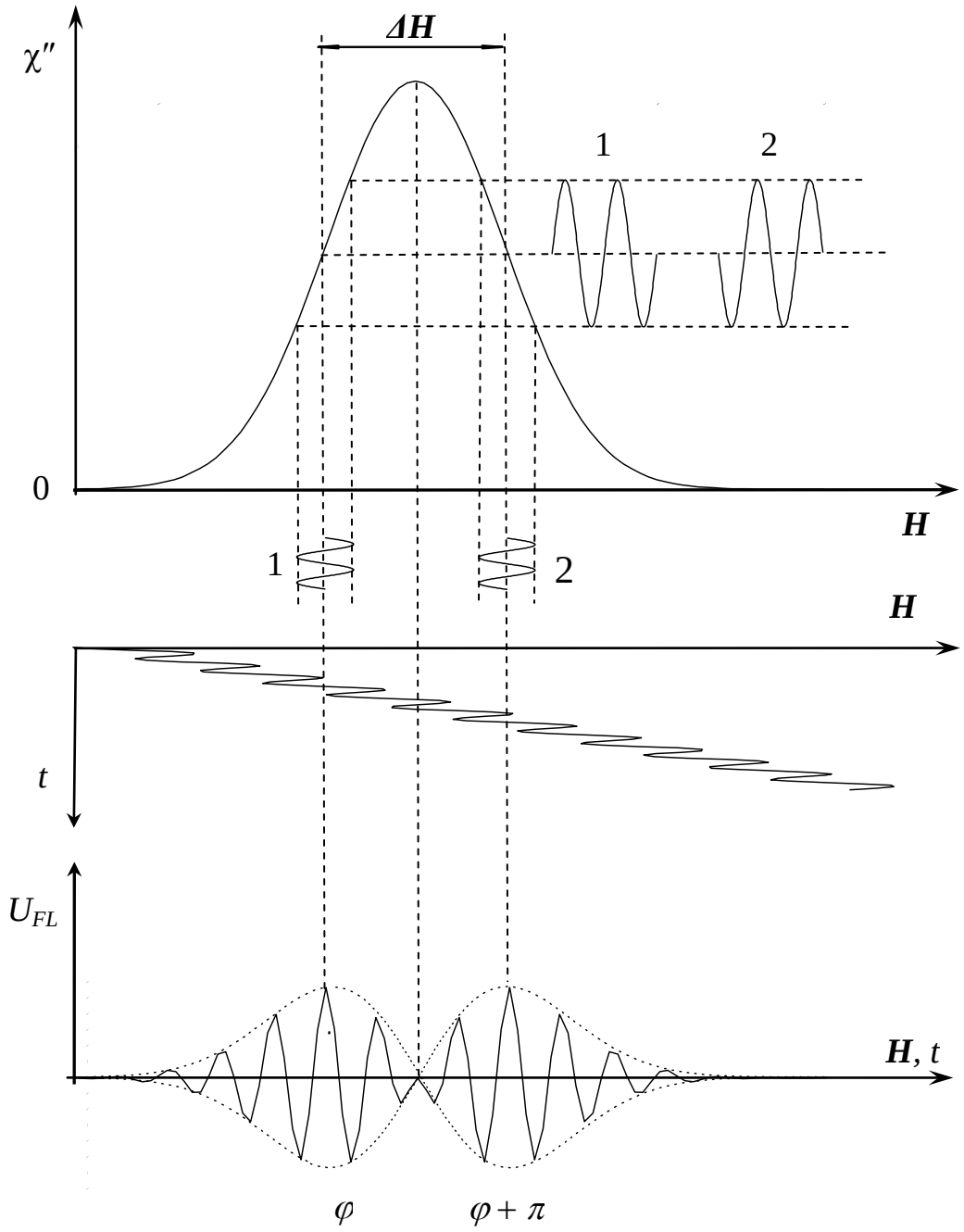

Fig. 6

The latter more often uses the double T-shaped RC-filter (Fig. 7) which passes all frequencies except the measured frequency (in our case except the modulation frequency Ω). As a result the negative feedback coupling operates on all frequencies except Ω, and in whole the device works as the resonance amplifier. Due to narrow transmission band of this amplifier the noise power on its output is essentially

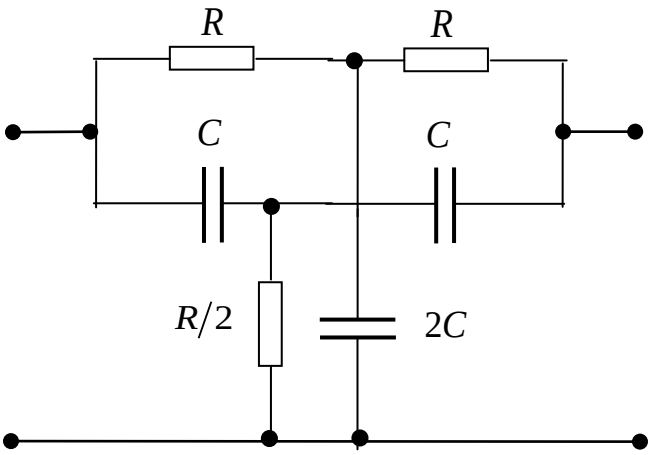

a)

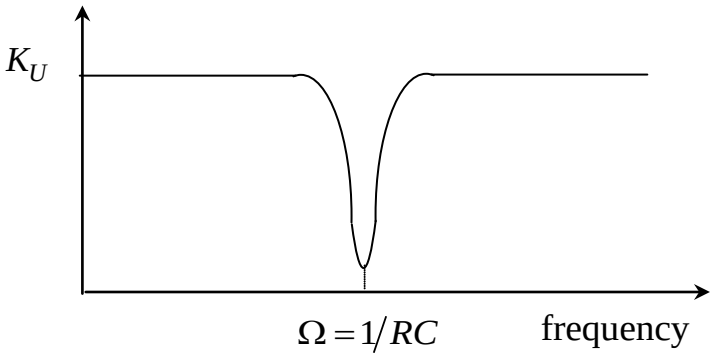

b)

Fig.7. Scheme (*a*) and frequency characteristic (*b*) of double T – shaped RC – filter

reduced, and this leads, in turn, to effective increase of the signal-to-noise ratio. Further increase of the signal-to-noise ratio is obtained by means of synchronous detection which appears possible due to that the useful signal has a narrow frequency spectrum near the fixed frequency Ω.

2.6. Lock-in detector

In lock-in detector the output voltage of the selective amplifier

$$u(t) = u_0 \sin \Omega t + e(t),$$

represents a mixture of the useful signal and noise $e(t)$, and is multiplied on the periodic function $F(t)$ with the period $\frac{2\pi}{\Omega}$ (reference voltage) and then is integrated over the time $2\tau >> \pi/\Delta\Omega$; here $\Delta\Omega$ – frequency spectrum width of signal $u(t)$, limited by pass bandwidth of the selective amplifier.

Let $F(t) = \sin\Omega t$. Then on the output of the lock-in detector we have:

$$\int_0^\tau u(t)\sin\Omega t\,dt = U(\tau) + E(\tau) = \frac{u_0\tau}{2}\left(1 - \frac{\sin 2\Omega t}{2\Omega t}\right) + E(\tau).$$

Since $\Omega\tau >> \Delta\Omega\tau >> 1$ the useful signal is equal to $u_0\tau/2$. The second term, due to noise, is a random quantity; therefore it is possible to speak only about the mean-square value $\left\langle E^2(\tau)\right\rangle$. The calculation results in expression:

$$\left\langle E^2(\tau)\right\rangle = \frac{\tau}{2}J(\Omega),$$

where $J(\Omega)$– spectral density of noise power at frequency Ω. This means that the noise passes through the synchronous detector as through the filter with the equivalent transmission band $2/\tau$. The signal-to-noise ratio at the output of the synchronous detector is:

$$\frac{U(\tau)}{\left\langle E^2(\tau)\right\rangle^{1/2}} = u_0\left[\frac{\tau}{2J(\Omega)}\right]^{1/2}$$

and it appears to be proportional to $\tau^{1/2}$, and, hence, can be made larger by increasing the integration time.

Fig. 8 shows the scheme of elementary lock-in detector with the field-effect (unipolar) transistor with two isolated gates. The integration time in the given scheme is determined by the time constant of a circuit $\tau = 2\pi \cdot RC$; by increasing *R* and *C* it is possible to achieve the equivalent transmission band of the synchronous detector of the order of few percent of hertz.

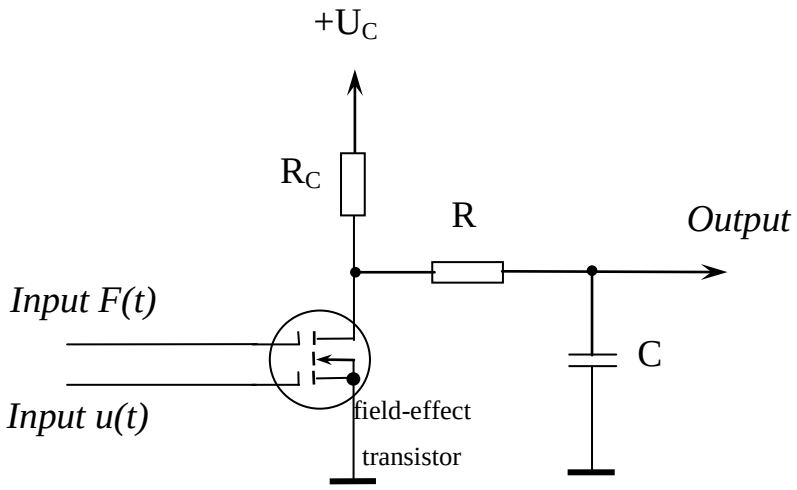

Fig. 8

Lock-in detector is also called a phase detector since a voltage on its output depends on phases of a signal and a reference voltage ratio. In fact, if the reference voltage is phase-shifted relative to signal on angle φ, then on the lock-in detector output we have:

$$U(\tau,\varphi)=\int_0^{\tau} u_0 \sin\Omega t\cdot\sin(\Omega t+\varphi)\,dt=$$

$$=\frac{u_0\tau}{2}\left\{\cos\varphi\left(1-\frac{\sin 2\Omega\tau}{2\Omega\tau}\right)-\sin\varphi\frac{\cos 2\Omega\tau}{2\Omega\tau}\right\}$$

or, since $\Omega\tau >> \Delta\Omega\tau >> 1$,

$$U(\tau,\varphi)=\frac{u_0\tau}{2}\cos\varphi.$$

A most simple way of input signal $u(t)$ multiplication with reference voltage $F(t)$ is the use of switch (for example, a diode switch). Then it is possible to present a reference voltage in the following form:

$$F(t)=\begin{array}{ll} -1, & -T/2<t<0,\\ +1, & 0<t<+T/2, \quad T=2\pi/\Omega\,. \end{array}$$

Expansion of this function in a Fourier series has the following form:

$$F(t) = \frac{4}{\pi} \sum_{n=0}^{\infty} \frac{\sin(2n+1)\Omega t}{2n+1}.$$

If $\Delta\Omega << \Omega$ then the noise spectrum on the synchronous detector output has no components with frequencies 3Ω, 5Ω, etc., therefore the terms of $F(t)$ with $n \neq 0$ do not give the contribution to the resulting signal.

3. Description of the experimental facility

3.1. Purpose of the spectrometer and its technical characteristics

The given laboratory work uses autodyne type broad line continious wave spectrometer intended for recording of NMR spectra in solids. The choice of nuclei for resonance observation is determined by magnetic field source of the spectrometer (permanent magnet) and practically limited to ^{19}F and ^{1}H isotopes. Recording of signals and postprocessing of spectra is performed by means of the microcontroller and tcomputer, respectively.

The spectrometer technical characteristics are as follows:

Operating frequencies of the autodyne generator … … … … ….5 – 40 MHz
Magnetic field … 2500 Oe
Modulation frequency … … … … … … … … … … … … … … … …. 373 Hz
Peak amplitude of magnetic field modulation … … … … … … … …. 50 Oe
Band of magnetic field scan … … … … … …… … … … 100 Oe
Voltage amplitude in the sample coil ... ... … … … … …. 50 – 500 mV
High frequency amplification gain... … … … … … … … … … … … 30 dB
LF-path amplification gain... … … … … … … … … … … … … … … 100 dB

3.2. Block diagram of facility and principle of operation

The spectrometer block diagram is shown in Fig. 9. The inductance coil with the sample is located in a bore of permanent magnet. For slow change of magnetic

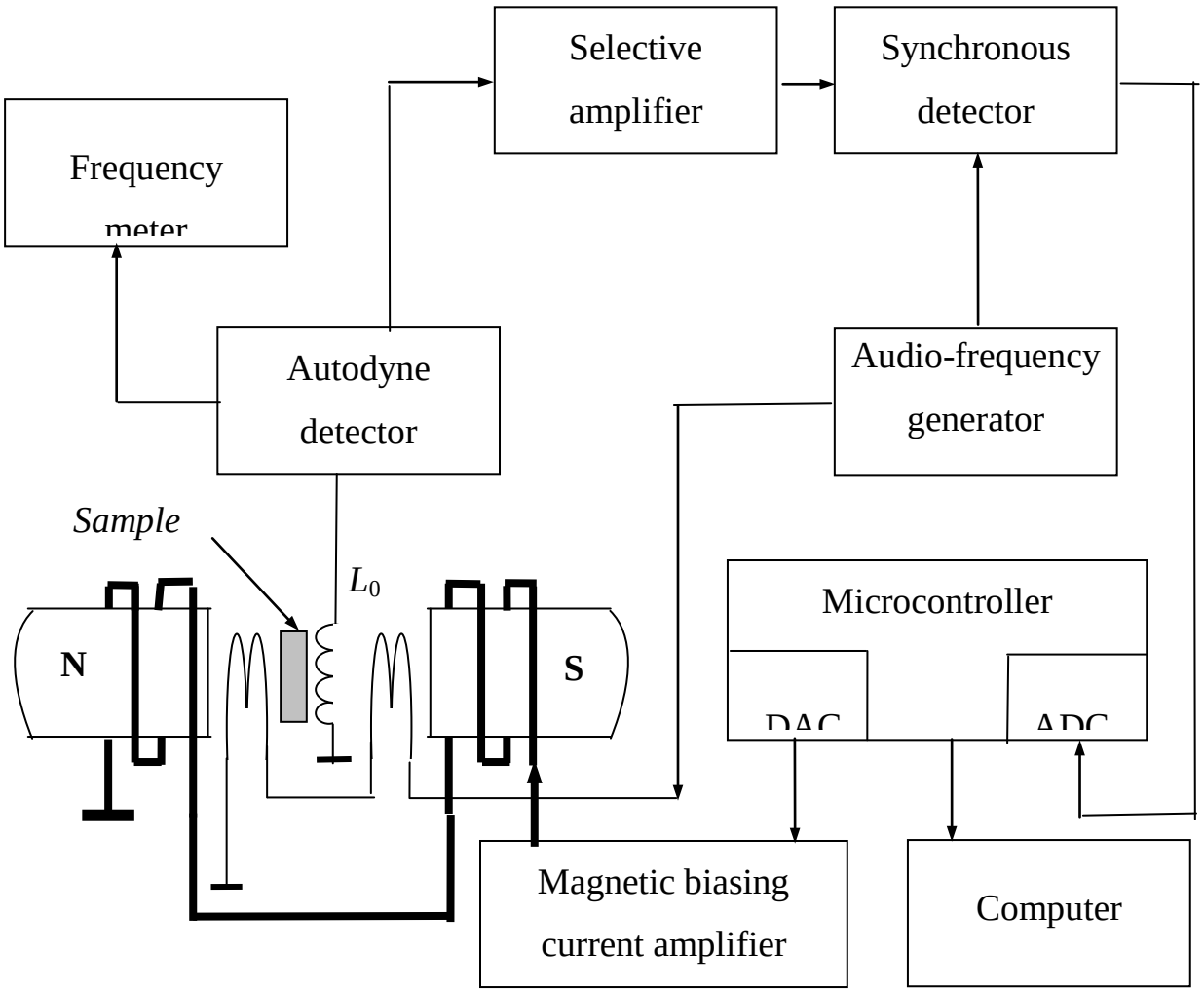

Fig. 9. Block diagram of spectrometer

field the coils for magnetic biasing shown by thick lines on the block diagram are used. The modulation coils are located in the immediate proximity of the sample.

The autodyne detector includes the diode amplitude detector of the high-frequency oscillations of the generator, which is applied to the input of the selective amplifier of the recording system, that amplifies the voltage with a frequency of 373 Hz. The amplified low-frequency voltage is applied to the input of the lock-in detector. The output voltage of audio-signal generator which simultaneously is applied to the modulation coils is used as a reference voltage of the lock-in detector.

The output of recording system is connected to input of analog-to-digital converter (ADC) of microcontroller ATMEGA 8535. Slow magnetic field scanning is carried out by the same microcontroller with the help of the digital-to-analog converter (DAC). Thus, for each measured point of NMR spectrum the

microcontroller sets the magnetic field intensity and measures the value of derivative of absorption signal. Then this data is transmitted to the computer and mapped on its screen in the form of NMR spectrum.

The autodyne detector is assembled according to the modified Pound-Knight scheme with two FET transistors KT312 (see Fig. 10). The first stage is common drain amplifier, second - common gate amplifier. The tank circuit is connected to the

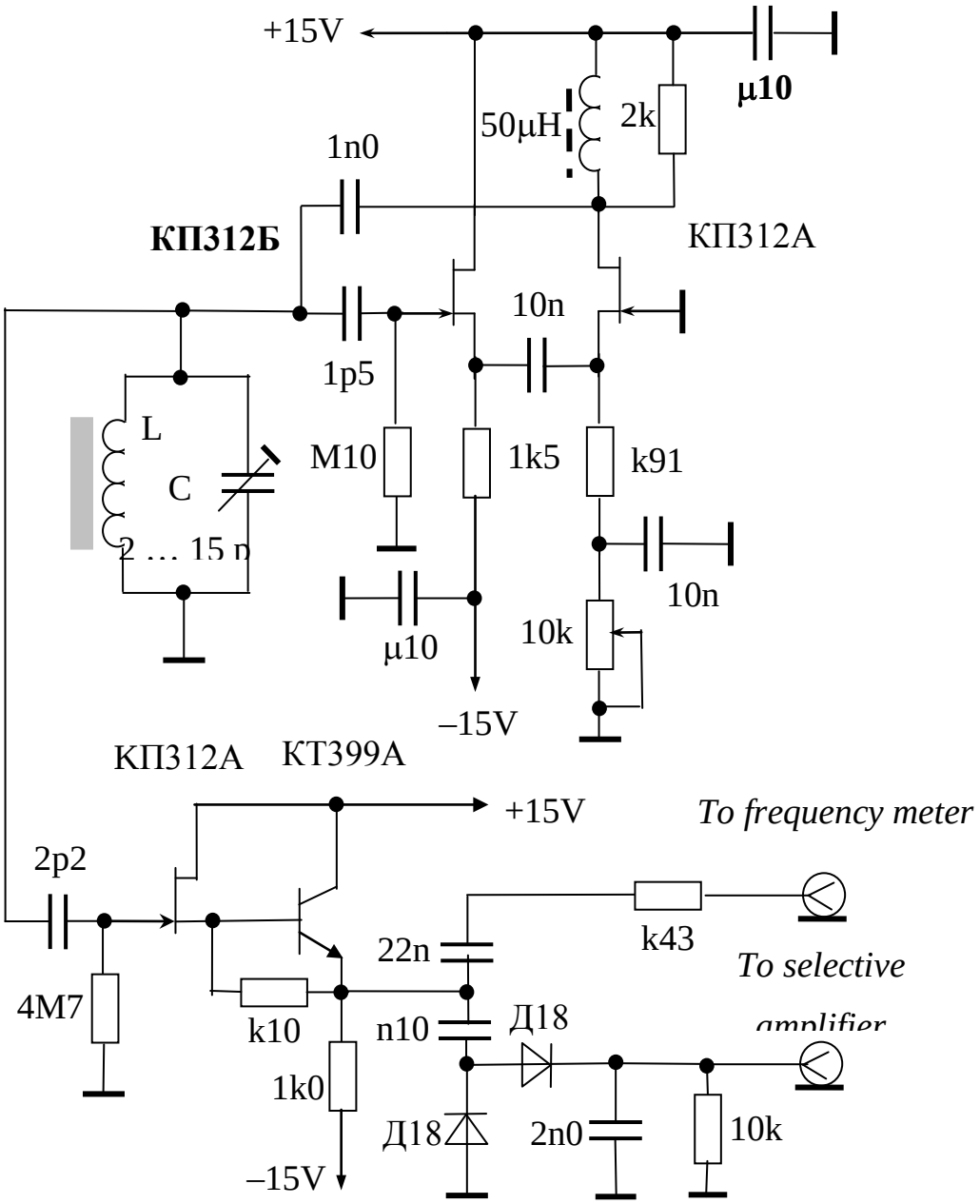

Fig. 10. Basic circuit of autodyne generator

first transistor gate (at the left) through a RC-circuit representing the high-pass filter, suppressing penetration of low-frequency voltage into the generator induced on the

coil because of magnetic field modulation. The oscillating mode is regulated by means of the variable resistor connected to the circuit of the second FET source. The current compensating the losses in the tank circuit, is applied to it through the capacitor (positive feed-back). The tank circuit is connected with high impedance input of the composite repeater (with field-effect transistor KP312A and bipolar transistor – KT 399A). Further, the signal is applied to the amplitude detector for the purpose of the subsequent lock-in detection, to frequency meter for the frequency control, and also to millivoltmeter input – indicator of oscillation level.

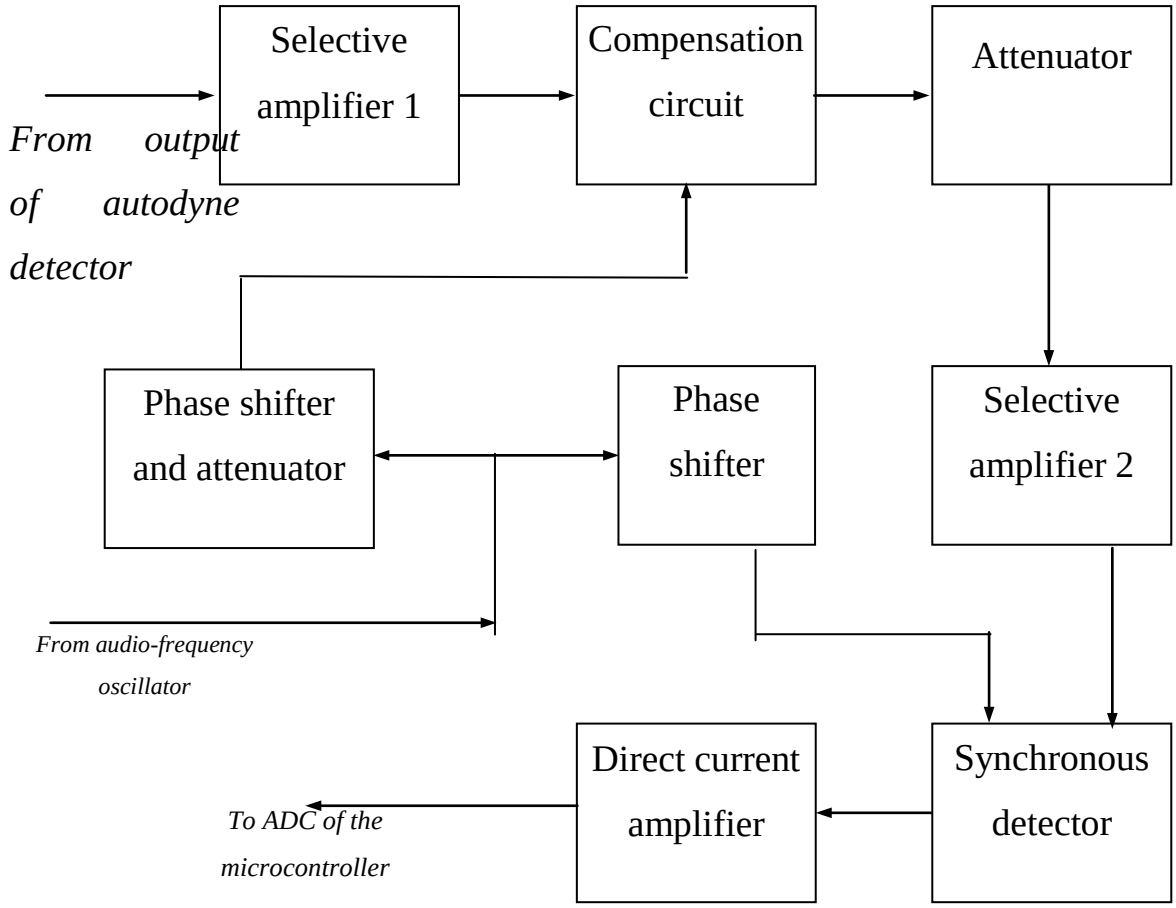

Fig. 11. Block diagram of the recording device

After amplitude detection the signal is applied to the recording device (see Fig. 11). Amplified by the selective amplifier, having the maximum amplification at the modulation frequency (373 Hz), it enters the compensation circuit of the spurious signal inevitably induced on the coil with the sample due to modulation of the magnetic field. The phase and amplitude of compensating voltage are selected so that in the absence of NMR signal there will be no voltage with frequency of 373 Hz at the circuit output. The compensation control is performed by Lissajous figures on the

oscilloscope screen, on which input X the reference voltage from the audio-frequency generator and on input Y – the output signal of the compensation circuit are applied. Then the basic selective amplifier is followed. The synchronous detector multiplies the amplified voltage together with reference voltage with the subsequent integration. The reference voltage phase is attuned so to obtain the maximum signal. The terminal stage of the recording scheme corresponds to direct-current amplifier which output is connected with ADC input of the microcontroller.

The principles of autodyne detection, double modulation and lock-in are described in detail in sections 2.4, 2.5, and 2.6.

4. Recording and processing of NMR spectra

Recording and processing of NMR spectra is carried out by the computer with the relevant software.

4.1. Program for NMR spectra recording

The window for recording program of NMR spectra is shown in Fig. 12.
The window contains the following elements:

1. Graphic information window;
2. “Start” – button for starting the magnetic field sweep;
3. “Stop” – button for stopping the magnetic field sweep;
4. “Save” – button for saving the measured spectrum;
5. “Freq” – window for input of NMR frequency;
6. “Quick” – switch button between the fast (for precheck) and slow magnetic field sweeps;
7. “Pause” – button for temporary stopping the field sweep;
8. “X” – current value of magnetic field in DAC units;
9. “Y ”– current value of NMR signal derivative;
10. “Dev”– window where the value of area of the NMR signal derivative is shown (for tuned spectrometer this value should be close to zero).

Procedure for operation with the software.

1. Tune the output of direct-current amplifier (in the recording device) on zero bias:

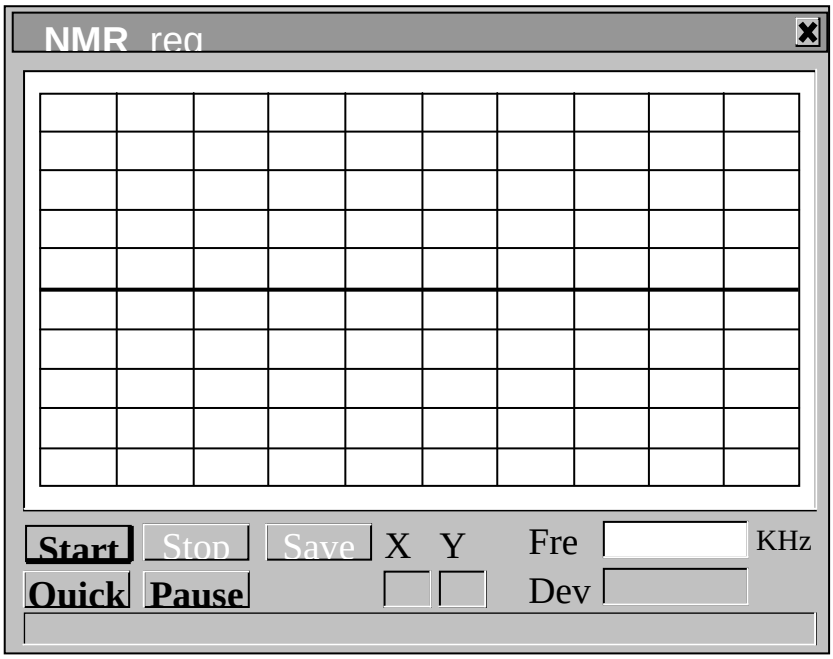

Fig. 12. Program window for NMR spectra recording

a) start magnetic field sweep and immediately stop it by button "Pause";

b) by rotating the bias controller of a direct-current amplifier achieve the value close to zero in window “Y”;

c) start field sweep by button "Pause" and immediately interrupt the record.

2. Start magnetic field sweep.

At the moment of magnetic field passage through the resonance conditions input into the window “Freq” the NMR frequency value measured by the frequency counter.

3. Stop recording and save the recorded spectrum into the folder [spectra].

4.2. The program for calculation of magnetic field values

It is very difficult to relate the voltage value at DAC output of the microcontroller and the magnetic field value in magnet bore since the magnetic field is affected by many parameters (for example, temperature of the magnet). Therefore, in order to determine the value of magnetic field, the possibility to record the NMR spectra at two slightly different frequencies is used.

Assume that we have recorded the NMR spectra at frequencies f_1 and f_2. After recording, it is possible to determine the positions of NMR lines for these two spectra, corresponding to two values of magnetic field intensity n_1 and n_2 which are given in some units (percent of scan value), not yet related with units of magnetic field intensity. On the other hand, knowing a gyromagnetic ratio γ, it is possible to determine the values of magnetic fields H_1 and H_2, corresponding to centers of two NMR spectra recorded at different frequencies: $H_i = f_i / \gamma$.

Now we can compare H_1 and H_2 with n_1 and n_2 and calculate in the linear magnetic field scan approach the value of magnetic intensity H for each point of the NMR spectrum with value n:

$$H = H_1 + \frac{H_2 - H_1}{n_2 - n_1}\left(n - n_1\right).$$

These calculations are carried out by the software for calculation of magnetic field values and its window is shown in Fig. 13.

Procedure for operation with the software.

1. Input, if it is necessary, the value of gyromagnetic ratio for nuclei of the corresponding ion into the window “gamma”.

2. Open with the button "Open" the main file with the data of NMR spectrum measured at frequency f_1. The spectrum will appear in the left part of the graph window. If it is necessary input the NMR frequency into the window “f_1”.

3. Open with a button "OpenFreq" file with the data of NMR spectrum measured at frequency f_2. The spectrum will appear in the right part of graph window. If it is necessary, input the NMR frequency into the window “f_2”.

4. Set with the computer mouse the red dashed lines on centers of NMR lines and press the button “Calculate H”. The abscissa axis of the main spectrum (left window) will be recalculated in magnetic field intensity values, and the spectrum saved into the same file with the new values of abscissa axis.

Let the other NMR spectra have been recorded together with that mentioned in

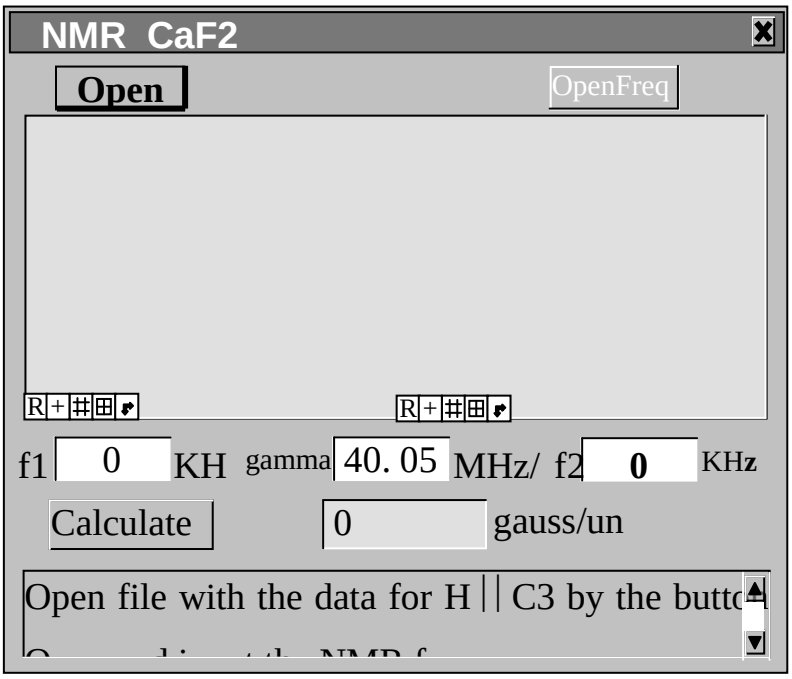

Fig. 13. Program window for calculation of magnetic field values

different conditions (for example, in different magnetic field orientation relative the crystal axes) at the same frequency f_1. Then by opening the corresponding file in the left part of graph window we will obtain a spectrum which abscissa axis will be automatically recalculated in magnetic field intensity units, and the program will automatically save the spectrum with new values of abscissa axis.

4.3. Program for extraction of the part of spectrum with the NMR line and line width evaluation

The parts of a spectrum that are located far away from the NMR line center do not contain any information about the line shape. However these parts as well as the whole spectrum contain the noise, which at evaluation of the second and the fourth moments of lines increase the error in estimations of the values of the moments. Therefore, to increase the measurement accuracy of the values of the moments it is necessary to use only the central part of a spectrum containing the NMR line, and the side parts of spectrum that contain only a noise should be removed. For this purpose the program for extraction of part of spectrum with NMR line and line width evaluation (see Fig. 14) is used.

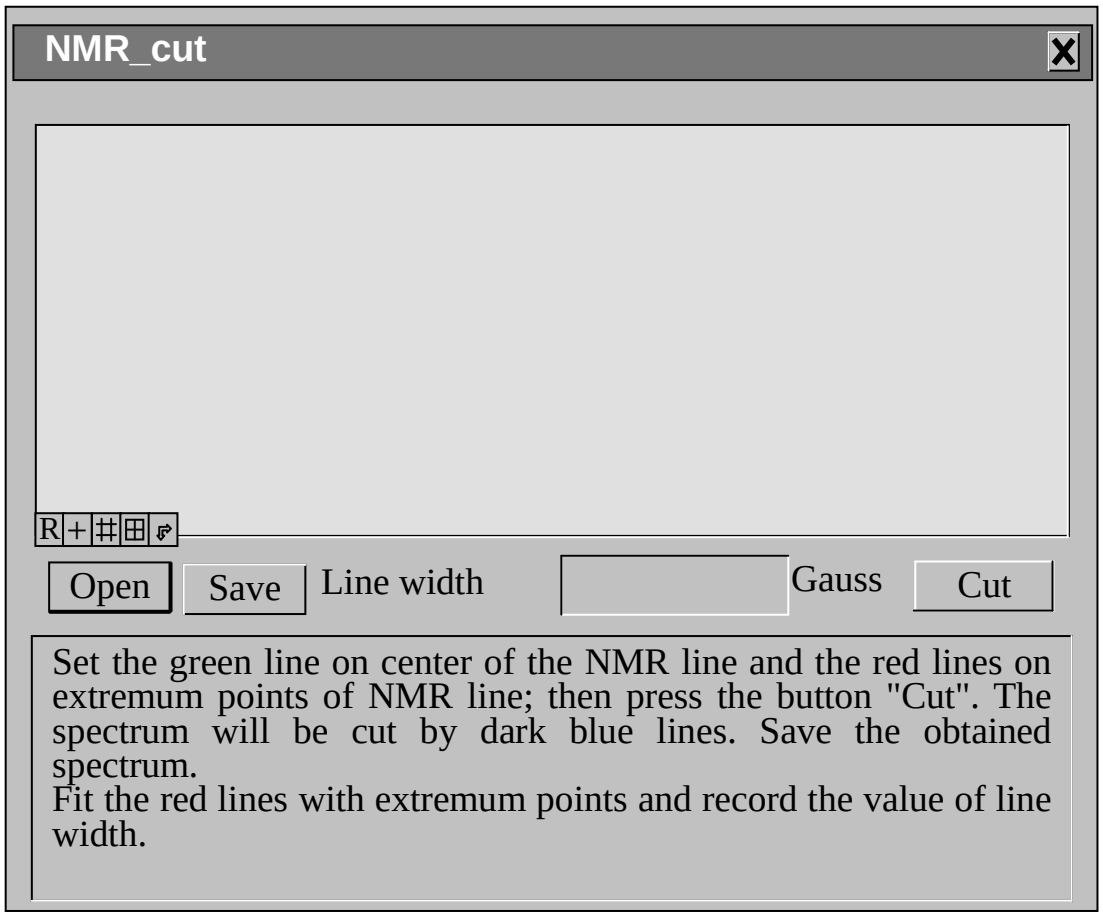

Fig. 14. Window of the program for extraction of part of spectrum with NMR absorption line and line width evaluation

Procedure for operation with the software.

1. Open a handled spectrum and set the green line on center of the NMR line derivative.

2. Set the red lines on extremum points of the NMR line derivative. The dark blue lines will simultaneously move and show the selected part of spectrum.

3. Cut the unnecessary parts of spectrum by button "Cut".

4. Save the obtained spectrum (button "Save").

5. Set again the red lines on extremum points and record the maximum value of the NMR line width.

Task

1. Familiarize yourself with principles of NMR theory in solids and methods of NMR signals detection (sections **1** and **2**).

2. Study the structural and electrical schematic diagram of NMR spectrometer (section **3**).

3. Record ^{19}F NMR lines in CaF_2 crystal at orientations of the static magnetic field along the crystallographic directions [100], [110] and [111] (in other notations C_4, C_2 and C_3, respectively).

4. Calculate the second and the fourth moments of the experimental curves; compare the obtained moments with the theoretical values (see equations (68), (71) and the **Appendix**); calculate the ratio M_4/M_2^2.

Appendix

A1. Data for CaF_2 crystal

Calcium fluoride CaF_2 belongs to space group O_h^5 and has the lattice constant a=5.46Å. Its structure can be viewed as a simple series of cubes formed by F^- ions with Ca^{2+} ions, being in the center of the every second cube. The crystal contains only one sort of ^{19}F nuclei with nonzero spin. The quadrupole effects are absent since

the nuclear ^{19}F spin is 1/2. The nuclei have large magnetic moments $\left(\mu = +2.63\,\mu_N,\ \gamma/2\pi = 4007\ \text{Hz/Oe}\right)$ and form a simple cubic lattice. The theoretical values of 4-th root of the fourth moment (in oersteds) for various directions of magnetic field relative the crystallographic axes are given below.

H Direction	[100]	[110]	[111]
$\sqrt[4]{M_4}$	4.31	2.73	1.88

A2. Evaluation of the moments from experimental curves

The calculation procedure of the moments from the experimental curves $\psi = \frac{d}{dH} f\left(H - \frac{\omega}{\gamma}\right)$ is reduced in essence to a double numerical integration and is explained by equations and Fig. 14 shown below.

Assuming that $H - \frac{\omega}{\gamma} = h$ we have:

$$M_n = \frac{\int_0^\infty h^n f(h)\,dh}{\int_0^\infty f(h)\,dh} = \frac{\sum_{m=1}^{N} (m\delta)^n \left(\frac{A_{m-1} + A_m}{2}\right)\delta}{\sum_{m=1}^{N} \left(\frac{A_{m-1} + A_m}{2}\right)\delta} = \frac{\sum_{m=1}^{N} (m\delta)^n \left(A_{m-1} + A_m\right)}{\sum_{m=1}^{N} \left(A_{m-1} + A_m\right)} =$$

$$= \delta^n \frac{\left(A_0 + A_1\right)\cdot 1^n + \left(A_1 + A_2\right)\cdot 2^n + \ldots + \left(A_{m-1} + A_m\right)\cdot m^n + \ldots + A_{N-1}\cdot N^n}{A_0 + 2\left(A_1 + A_2 + \ldots + A_{N-1}\right)}.$$

$$A_N = 0;\ A_{N-1} = a_{N-1}\cdot\delta;\ A_{N-2} = A_{N-1} + a_{N-2}\cdot\delta;$$

$$A_{N-3} = A_{N-2} + a_{N-3}\cdot\delta;\ \ldots;\ A_1 = A_2 + a_1\cdot\delta;\ A_0 = A_1 + a_0\cdot\delta.$$

For correct approximation of absorption curve the interval δ should be small enough: the value of N should be of the order of 15 … 30.

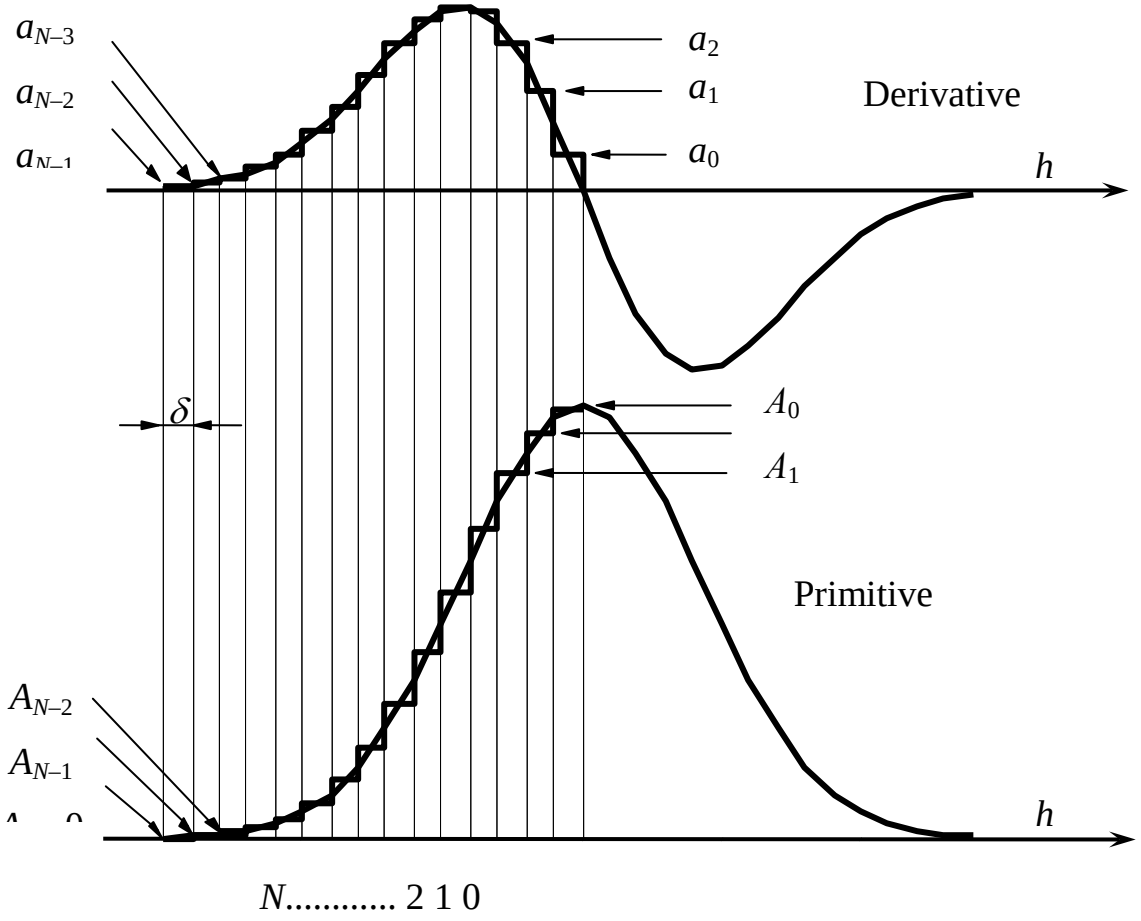

Fig. 15

PART 2
PULSED NUCLEAR MAGNETIC RESONANCE IN SOLIDS

1. Classical description of pulsed nuclear magnetic resonance

1.1. Motion of noninteracting spins

The mechanical ($\mathbf{J}$) and magnetic ($\boldsymbol{\mu}$) moments of nuclei are related through the following relation $\boldsymbol{\mu} = \gamma \mathbf{J}$, where γ – scalar value called the gyromagnetic ratio. Interaction of the magnetic moment with a static magnetic field $\mathbf{H}_0$ causes the mechanical moment precession. The equation of motion for magnetic moment can be written as follows:

$$d\mathbf{J}/dt = \boldsymbol{\mu} \times \mathbf{H}_0, \quad d\boldsymbol{\mu}/dt = \boldsymbol{\mu} \times \gamma \mathbf{H}_0$$

Or, finally, $d\boldsymbol{\mu}/dt = \boldsymbol{\omega}_0 \times \boldsymbol{\mu}$.

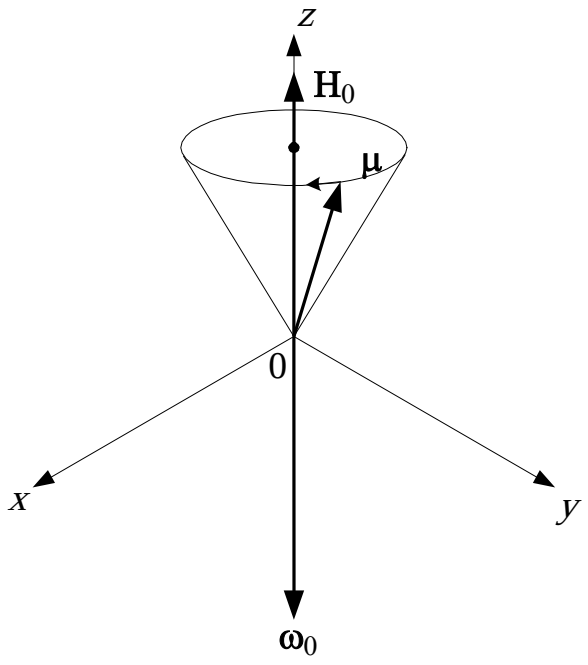

Fig. 1. Precession of moment in the magnetic field

The angular velocity $\boldsymbol{\omega}_0 = -\gamma \mathbf{H}_0$ (precession frequency $\omega_0 = |\boldsymbol{\omega}_0| \equiv \gamma H_0$) is called a Larmor frequency.

If the magnetic field is applied along the axis *z* the precession will occur as it is shown in Fig. 1, in the direction of arrow, with a Larmor frequency; the magnetic moment delineates a cone.

The given equation of motion is written in the fixed coordinate system which is also called a laboratory frame (LF).

1.2. Rotating frame (RF)

When considering a magnetic resonance it is convenient to use rotating frame The latter has some angular velocity relative the laboratory frame. It is obvious that if RCS rotates with the Larmor precession velocity the magnetic moment in this coordinate system will be fixed. We will show this. Consider some vector function of time $\mathbf{F}(t) = \mathbf{i}F_x + \mathbf{j}F_y + \mathbf{k}F_z$, where **i**, **j**, **k** – the unit vectors directed along the Cartesian coordinates, rotating with angular velocity **Ω**. Then for these vectors the following equations are valid:

$$d\mathbf{i}/dt = \mathbf{\Omega} \times \mathbf{i},$$
$$d\mathbf{j}/dt = \mathbf{\Omega} \times \mathbf{j},$$
$$d\mathbf{k}/dt = \mathbf{\Omega} \times \mathbf{k}.$$

The total time derivative of function **F** is equal to:

$$\frac{d\mathbf{F}}{dt} = \mathbf{i}\frac{dF_x}{dt} + \mathbf{j}\frac{dF_y}{dt} + \mathbf{k}\frac{dF_z}{dt} + F_x\frac{d\mathbf{i}}{dt} + F_y\frac{d\mathbf{j}}{dt} + F_z\frac{d\mathbf{k}}{dt} =$$
$$= \mathbf{i}\frac{dF_x}{dt} + \mathbf{j}\frac{dF_y}{dt} + \mathbf{k}\frac{dF_z}{dt} + \mathbf{\Omega} \times \left(\mathbf{i}F_x + \mathbf{j}F_y + \mathbf{k}F_z\right).$$

The first three terms represent the derivative of function in RF. We will designate it as $\frac{\delta \mathbf{F}}{\delta t}$. Then $\frac{\delta \mathbf{F}}{\delta t} = \frac{d\mathbf{F}}{dt} - \mathbf{\Omega} \times \mathbf{F}$.

Thus, the equation of motion for magnetic moment in a coordinate system rotating with frequency ω may be written as

$$\frac{d\boldsymbol{\mu}}{dt} = \boldsymbol{\mu} \times \gamma\mathbf{H}_0 - \boldsymbol{\omega} \times \boldsymbol{\mu} = \boldsymbol{\mu} \times \left(\gamma\mathbf{H}_0 + \boldsymbol{\omega}\right)$$

(hereinafter we will use a usual designation for derivative of vector quantity, stipulating thus what coordinate system is used). Really, if $\boldsymbol{\omega} = -\gamma\mathbf{H}_0 \equiv \boldsymbol{\omega}_0$, then $\frac{d\boldsymbol{\mu}}{dt} = 0$, and the precession is absent. It is possible to imagine that in RF the precession is caused by the effective magnetic field, $\frac{d\boldsymbol{\mu}}{dt} = \boldsymbol{\mu} \times \gamma\mathbf{H}_{eff}$, where $\mathbf{H}_{eff} = \mathbf{H}_0 + \boldsymbol{\omega}/\gamma$, and absence of precession is a consequence of zero effective field.

In macroscopical object the spins precess with arbitrary phase, therefore the total moment $\mathbf{M} = \sum \boldsymbol{\mu}_i$ is directed parallel to magnetic field $\mathbf{H}_0$ as shown in Fig. 2 and the equation for its motion in RF has the same form as for the individual moment – spin:

$$\frac{d\mathbf{M}}{dt} = \mathbf{M} \times \gamma \mathbf{H}_{eff}.$$

Suppose that except a field $\mathbf{H}_0 = H_0\mathbf{k}$ there is a transverse field $\mathbf{H}_1 = H_1\mathbf{i}$ directed along the x -axis of RF. This means that in LF it rotates with a frequency ω in direction of precession. In this case the effective field $\mathbf{H}_{eff} = \left(H_0 - \omega/\gamma\right)\mathbf{k} + H_1\mathbf{i}$, around which there is a magnetization precession (Fig. 3), is not zero even in the case when $\omega = \omega_0$, and, hence, it is possible to create transverse magnetization, affecting by rather weak rotating magnetic field with a frequency close to the Larmor frequency. This is called a magnetic resonance. In practice one inductance coil is usually used for observation of nuclear magnetic resonance (NMR). At alternating current flow through it there causes a linearly polarized alternating magnetic field $2H_1 \cos\omega t$ directed along the coil axis.

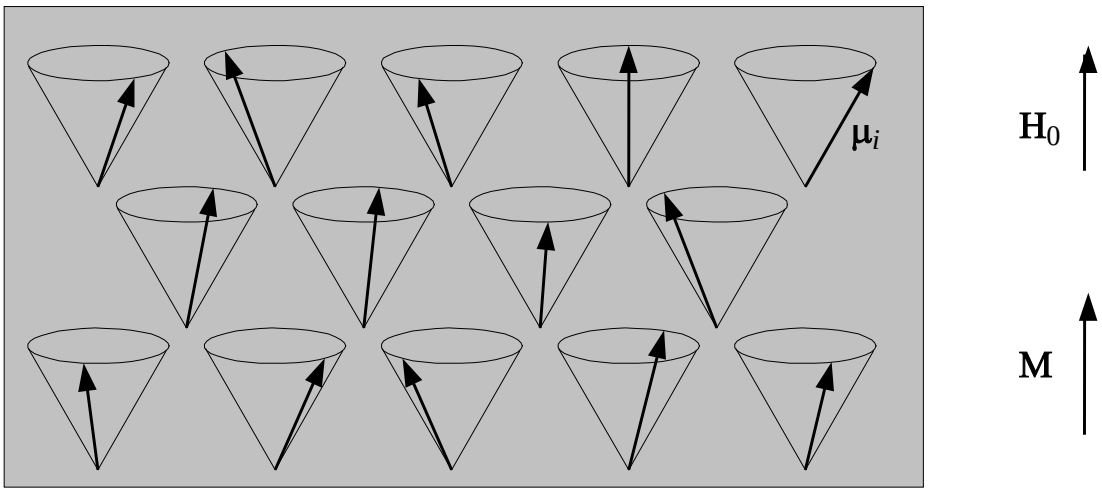

Fig. 2. Magnetic moments in the sample in equilibrium state.
Transverse magnetization is absent.

Nevertheless, all reasons given above remain valid, as it is possible to present it in the form of sum of two rotating fields with value H_1 but with frequency ω in opposite directions, as shown in Fig. 4.

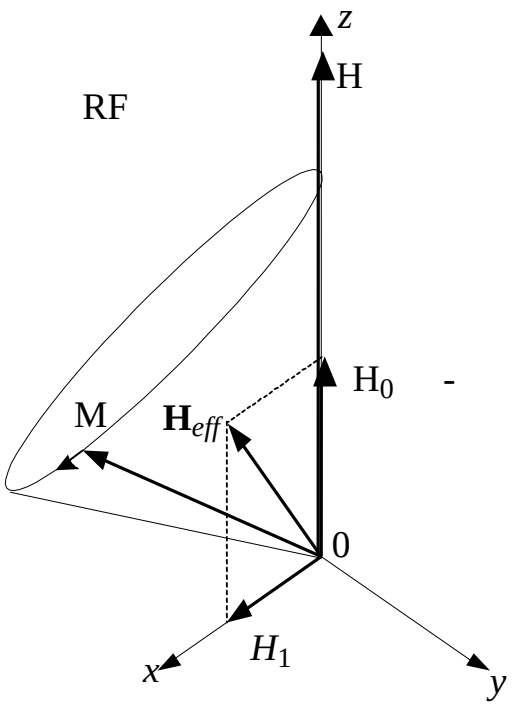

Fig. 3. Magnetization precession in RCS in the presence of variable field.

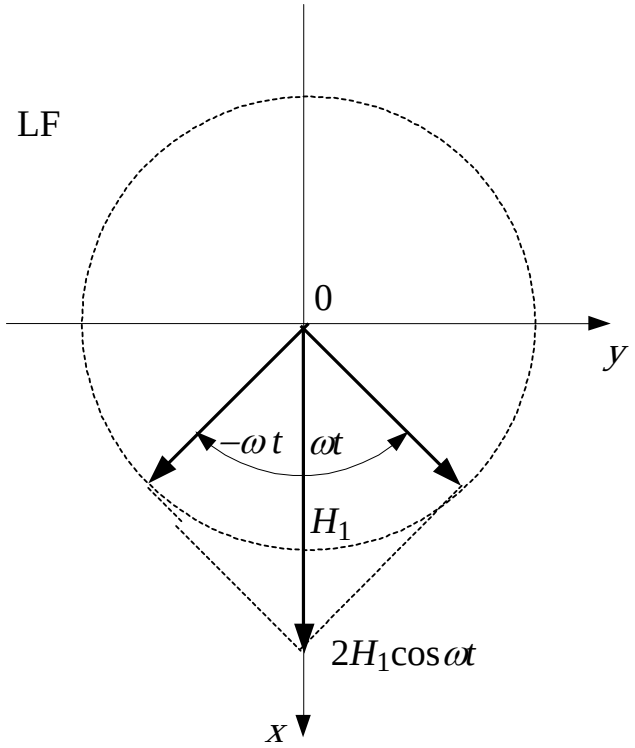

Fig. 4. Decomposition of linearly polarized field on two rotating fields.

The component which rotates in direction opposite to the precession direction (on the right in Fig. 4) may be neglected. Really, if $\omega \approx \omega_0$ and $H_1 << H_0$ then the effective field in this case is $\mathbf{H}_{eff} = \left(H_0 + \omega/\gamma\right)\mathbf{k} + H_1\mathbf{i} \approx 2H_0\mathbf{k}$, and this component would not affect the magnetization.

1.3. Free induction decay (FID)

In pulsed NMR methods alternating (radio-frequency – RF) field is applied for short period of time – in the form of a pulse. If we consider the case of exact resonance $\omega = \omega_0$ then the effective field $\mathbf{H}_{eff} = H_1\mathbf{i}$, and the magnetization rotates

with angular velocity $\omega_1 = \gamma H_1$ around the axis *x*. To obtain the maximum transverse magnetization a rotation by $\pi/2$ angle is required. The pulse, causing such an effect, is called $\pi/2$- pulse. Its duration τ should satisfy the requirement $\omega_1 \tau = \pi/2$. As a result the magnetization appears directed along the *y* -axis of RF, as shown in Fig. 5.

The magnetization static in RF rotates relative the inductance coil with Larmor frequency and creates alternating magnetic field. As a result an induction electromotive force (EMF) on the coil turns is induced that is proportional to $\omega_0 M$, which can be registered by radio engineering methods. The alternating voltage on the coil, created due to nuclear induction, was called free induction decay – FID. This voltage gradually damps due to not exactly equal frequencies of precession of different groups of spins that can be caused by both heterogeneity of a static magnetic field and the local fields, which are created by spins (spin-spin interaction). This process was called the transverse relaxation. Besides, due to spin-lattice (longitudinal) relaxation the spin-system is returned to equilibrium state in which there is only a longitudinal magnetization. It is generally accepted to designate these time constants, characterizing these two processes, as T_2 and T_1 , respectively.

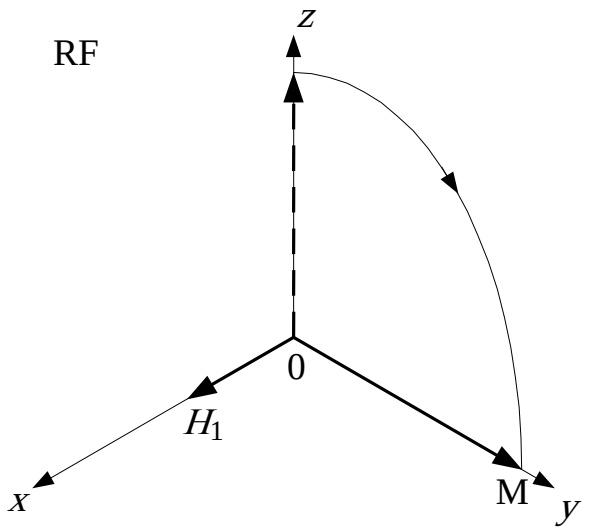

Fig. 5. Creation of transverse magnetization with the help of $\pi/2$-pulse.

1.4. Spin echo

The classical vector model allows us to explain the spin echo phenomenon. Its essence is that if we apply one more pulse after the time period τ ($\tau > T_2$) after $\pi/2$ pulse, twice longer in duration compared with the first one, then at the time 2τ the broken transverse magnetization will appear again (see Fig. 6). Supposing that the origin of transverse magnetization decay is the dispersion of Larmor frequencies of

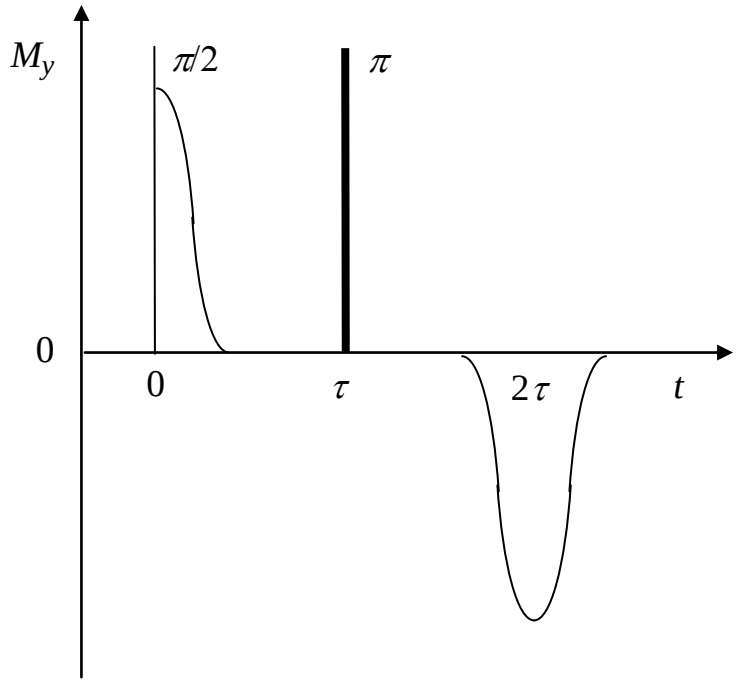

Fig. 6. Spin echo.

different groups of spins – spin packets, it is possible to explain the mechanism of echo occurrence by considering the behavior of magnetizations of the two spin packets with Larmor frequencies $\omega_{1,2} = \omega_0 \pm \Delta\omega$. For the time τ the magnetization will deviate from the y -axis of RF on angles ($\pm\Delta\omega\tau$ Fig. 7a). Then the second pulse will turn both magnetizations on angle π around the axis x (Fig. 7b), the precession direction thus, naturally, will not change. As a result both magnetizations will converge to the axis $-y$ with the same angular velocity as that deviated from the y axis. In time τ after the second pulse they will merge. Since this reasoning is valid for any spin packet, then at the time moment 2τ the transverse magnetization will be completely recovered.

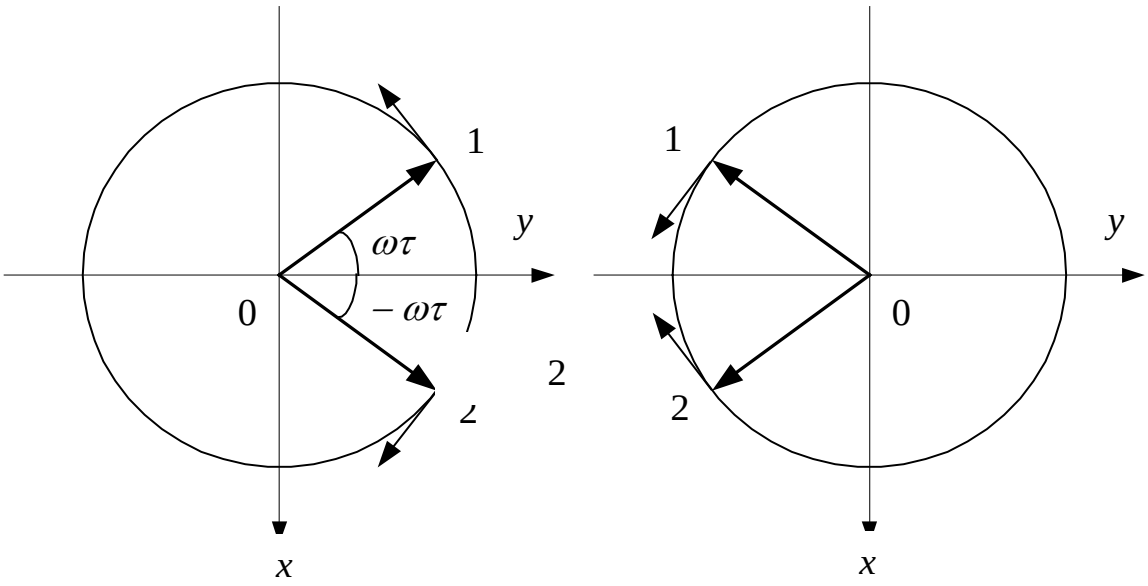

а) б)

Fig. 7. Values of magnetizations of two spin packets with Larmor frequencies $\omega_{1,2} = \omega_0 \pm \Delta\omega$ before (a) and after (b) π pulse.

2. Quantum-mechanical treatment of pulsed nuclear magnetic resonance

2.1. Equation of motion

Interaction of spin with a magnetic field is described by the energy operator, the Hamiltonian $\mathsf{H} = -\gamma \mathsf{h}\mathbf{HI}$, where $\mathbf{I}$ – spin operator. Proceeding from the Schroedinger equation it is possible to obtain the equation of motion of any observable value (including magnetic moment). Suppose that the wave functions $\mathbf{\Psi}$ and $\mathbf{\Phi}$ satisfy the Schrodinger equation:

$$-\frac{\mathsf{h}}{i}\frac{\partial \Psi}{\partial t} = \mathsf{H}\Psi; \quad -\frac{\mathsf{h}}{i}\frac{\partial \Phi}{\partial t} = \mathsf{H}\Phi;.$$

Then for any operator F it is possible to write the equation

$$\frac{d}{dt}\int \Psi^* \mathbf{F}\,\Phi d\tau = \int \frac{\partial \Psi^*}{\partial t}\mathbf{F}\,\Phi\, d\tau + \int \Psi^* \mathbf{F}\frac{\partial \Phi}{\partial t} d\tau =$$
$$= \int \frac{i}{\hbar}\left(\mathsf{H}\Psi\right)^* \mathbf{F}\,\Phi d\tau - \int \frac{i}{\hbar}\Psi^* \mathbf{F}\,\mathsf{H}\Phi d\tau = \frac{i}{\hbar}\int \Psi^* \left(\mathsf{H}\mathbf{F} - \mathbf{F}\mathsf{H}\right)\Phi\, d\tau,$$

or $\frac{d\mathbf{F}}{dt} = \frac{i}{\hbar}\left[\mathsf{H}, \mathbf{F}\right]$ since this is true for any matrix elements of F. At derivation we used the relation $\left(\mathsf{H}\Psi\right)^* = \Psi^* \mathsf{H}$ valid for Hermitian operators.

It is easy to be convinced that the obtained equation is equivalent to classical one if we choose the nuclear spin as operator, and the Hamiltonian describes the Zeeman interaction:

$$\mathbf{F} = \mathbf{i}I_x + \mathbf{j}I_y + \mathbf{k}I_z \;,\; \mathsf{H} = -\gamma\hbar\left(H_x I_x + H_y I_y + H_z I_z\right).$$

2.2. Statistical ensemble of noninteracting spins.

Is it possible to describe the ensemble comprised of N identical noninteracting spins in a magnetic field by means of the wave function of one spin N? We will try to do it supposing that the spin is equal to $1/2$. We will write the wave function in the form of superposition of "pure" wave functions: $\psi = a_1\xi + a_2\eta$, $\left|a_1\right|^2 + \left|a_2\right|^2 = 1$, ξ corresponds to the spin aligned along a field, and η – backwards. Then the components of macroscopic magnetization of ensemble are determined by the following expressions:

$$\frac{M_x}{\gamma\hbar} = N\left\langle I_x \right\rangle = \frac{1}{2}N\left[a_1^* a_2 + a_2^* a_1\right],$$
$$\frac{M_y}{\gamma\hbar} = N\left\langle I_y \right\rangle = \frac{i}{2}N\left[a_1^* a_2 - a_2^* a_1\right],$$
$$\frac{M_z}{\gamma\hbar} = N\left\langle I_z \right\rangle = \frac{1}{2}N\left[\left|a_1\right|^2 - \left|a_2\right|^2\right].$$

The last equality seems obvious if we consider that $\left|a_1\right|^2$ and $\left|a_2\right|^2$ are the relative densities of level populations. However, from the first two expressions it follows that the transverse magnetization is equal to zero only if $a_1 = 0$ or $a_2 = 0$, that is in case of the full polarization of spins, that does not represent the facts. So, the assumption that knowledge of one-particle wave function for the description of ensemble of spins appeared to be untenable. To determine the transverse magnetization the ensemble averages of products of coefficients: $\overline{a_1^* a_2} = \frac{1}{N}\sum_{i=1}^{N} \overline{a_1^{*i} a_2^i}$ shall be considered. For the most complete description of spin system including the presence of interaction, knowledge of all such products is required. The latter are the elements of density matrix ρ. The total number of spin system states is equal to $(2I+1)^N$, hence, the size of density matrix is $(2I+1)^N \times (2I+1)^N$ and its elements are equal to $\rho_{m,m'} = \langle m|\rho|m'\rangle = a_m^* a_{m'}$.

If the density matrix is known it is possible to determine the average value of any observable quantity: $\langle Q\rangle = Sp\{\rho Q\}$. The time dependence of density matrix is described by the equation

$$\frac{\hbar}{i}\cdot\frac{d\rho}{dt} = -[\mathsf{H},\rho].$$

In case if the Hamiltonian is time independent the solution of the equation is

$$\rho(t) = e^{-i\frac{\mathsf{H}}{\hbar}t}\rho(0)e^{i\frac{\mathsf{H}}{\hbar}t}.$$

It is most simple to write the equilibrium density matrix in proper representation of the Hamiltonian H. If we designate the energy values as $E_i = \langle i|\mathsf{H}|i\rangle$, then the nondiagonal elements of density matrix are equal to zero, and the diagonal elements $(\rho_0)_{ii} = e^{-E_i/kT} \Big/ \sum_{i=1}^{(2I+1)^N} e^{-E_i/kT}$ are equal to energy level populations according to the Boltzmann statistics.

2.3. Free induction decay and spin echo

The density matrix formalism allows to explain a free induction decay and spin echo phenomena. We will write the equilibrium density matrix for system of N spins I: $\rho_0 \propto e^{\mathsf{H}/kT}$, where H – main Hamiltonian that describes the interaction of spins with the magnetic field, $\mathsf{H} = -\gamma \mathsf{h} H_z I_z$, $I_z = \sum_{i=1}^{(2I+1)^N} I_z^i$. In the high-temperature approach ($\mathsf{H} << kT$) it is possible to expand the density matrix into a series and constrain with the first term of expansion $e^{-\mathsf{H}/kT} \cong \mathbf{1} - \mathsf{H}/kT$, where $\mathbf{1}$ – unit matrix (operator). Neglecting the latter, we will finally write $\rho_0 \propto I_z$.

The effect of variable magnetic field on a density matrix and also its evolution are described by means of exponential operators. One can show that the operator $e^{-i\theta I_x}$ turns the spin operators on angle θ around the axis x, i.e. after the effect of $\pi/2$ pulse $e^{-i\frac{\pi}{2}I_x} I_z e^{i\frac{\pi}{2}I_x} = I_y$.

In the event when the decay of transverse magnetization occurs due to a dipole-dipole interaction of nuclear spins, further evolution of density matrix goes on according to the following law:

$$\rho(t) = e^{-i\frac{\mathsf{H}'}{\mathsf{h}}t} I_y e^{i\frac{\mathsf{H}'}{\mathsf{h}}t},$$

where H' – secular part of the dipole-dipole interaction. (About the origins of truncation of the Hamiltonian of dipole interaction see the description of laboratory work “Continuous nuclear magnetic resonance in solids”). Thus, the transverse magnetization will depend on time as

$$M_y(t) \propto Sp\{\rho I_y\} = Sp\left\{e^{-i\frac{\mathsf{H}'}{\mathsf{h}}t} I_y e^{i\frac{\mathsf{H}'}{\mathsf{h}}t} I_y\right\} = G_1(t).$$

We note that the latter expression is written in RF rotating with frequency $\omega_0 = \gamma H_z$ and describes the free induction decay (FID) – a signal of pulsed NMR related to a CW signal $f(\omega)$ by the Fourier-transform:

$$f(\omega) = \int_{-\infty}^{+\infty} G_1(t) \cos \omega t \, dt .$$

In the case when the magnetic field heterogeneity is the origin of NMR line broadening it is possible to demonstrate the occurrence mechanism of spin echo. The density matrix after a $\pi/2$ pulse is also equal to I_y. The Hamiltonian of Zeeman interaction of spins in a rotating coordinate system can be written as $\mathsf{H} = -\mathsf{h}\sum \Delta\omega_i I_z^i$, where $\Delta\omega_i = \gamma H_i - \omega_0$, and H_i – magnetic field in the location of i th spin. Then, at the time $t = \tau$,

$$\rho(\tau) = e^{\tau \sum \Delta\omega_i I_z^i} I_y e^{-\tau \sum \Delta\omega_i I_z^i} .$$

If at this time a π pulse is applied, then after it

$$\rho(\tau_+) = e^{-i\pi I_x} e^{\tau \sum \Delta\omega_i I_z^i} I_y e^{-\tau \sum \Delta\omega_i I_z^i} e^{i\pi I_x} = e^{-\tau \sum \Delta\omega_i I_z^i} \left(-I_y\right) e^{\tau \sum \Delta\omega_i I_z^i} .$$

Further change of density matrix goes on as

$$\rho(\tau + t') = e^{t' \sum \Delta\omega_i I_z^i} e^{-\tau \sum \Delta\omega_i I_z^i} \left(-I_y\right) e^{\tau \sum \Delta\omega_i I_z^i} e^{-t' \sum \Delta\omega_i I_z^i} .$$

It is clear that when $t' = \tau$ (at the time $t = 2\tau$), then $\rho(2\tau) = -I_y$. This means that transverse magnetization recovered, but has changed its sign as it follows also from the classical model.

3. Nuclear spin-lattice relaxation

At low temperatures (and often at room temperature also) the observable relaxation times are much shorter compared with that might be expected. The only way to explain a relaxation is the assumption that even the purest crystals contain the paramagnetic impurities. The nuclei relax by interacting with their electronic spins which in turn relax into a lattice following the one of the mechanisms considered previously.

3.1. Random field model

If the diamagnetic ion with the paramagnetic nucleus is located near the paramagnetic ion then there is an interaction between them which can be generally written as:

$$\hat{H}_{SI} = \mathbf{S} \cdot \hat{A} \cdot \mathbf{I}.$$

If the ion and nucleus are located sufficiently far from each other so the density of electronic wave function on the nucleus is equal to zero, then the electron – nucleus interaction is the pure dipole interaction (interaction of two dipoles):

$$a_{ij} = \frac{\gamma_S \gamma_I \hbar^2}{r^3}\left(\mathbf{I}_i \mathbf{S}_j - 3\frac{(\mathbf{I}_i \cdot \mathbf{r}_{ij}) \cdot (\mathbf{S}_j \cdot \mathbf{r}_{ij})}{r_{ij}^2} \right).$$

The transitions between the nucleus levels, i.e. a nucleus relaxation, can be caused by the magnetic field fluctuations created by the electronic spin on a nucleus. These fluctuations can arise due to change of $\hat{A} = \hat{A}(t)$, for example as a result of electron – nucleus distance change (relaxation of the 1st type), or due to change of vector of a spin with time $\mathbf{S} = \mathbf{S}(t)$, for example due to spin orientation $\mathbf{S}$ change with time due to electronic relaxation.

Anyway it is possible to present the electron-nuclear interaction as follows: $\hat{H}_{SI} = -\gamma_I \mathsf{h} \cdot \mathbf{H}_e \cdot \mathbf{I}$, where $\mathbf{H}_e = \mathbf{H}_e(t)$ - magnetic field created by the electronic spin on a nucleus.

The spectral density of the fluctuating field created by the electronic spin on a nucleus is:

$$J(\omega) = \int_{-\infty}^{\infty} < H_e(t) \cdot H_e(t-\tau) > \exp(-i\omega\tau)\, d\tau\,,$$

where $H_e(t) \cdot H_e(t-\tau)$ – correlation function of fluctuations, <…> – average at the given temperature.

If we write $\hat{H}_{SI}$ in a coordinate system where the axis z || $\mathbf{H}_0$ (external field), introduce the angles Θ and φ setting the vector **r** connecting a nucleus and an electron, then we will obtain:

$$\hat{H}_{SI} = \hat{A} + \hat{B} + \hat{C} + \hat{D} + \hat{E} + \hat{F},$$

$$\text{where } \hat{A} \sim S_z I_z;\ \hat{B} \sim (S_+ I_- + S_- I_+);\ \hat{C} \sim (S_z I_+ + S_+ I_z);$$

$$\hat{D} \sim (S_z I_- + S_- I_z);\ \hat{E} \sim S_+ I_+;\ \hat{F} \sim S_- I_-.$$

We will assume that the distance between the nucleus and the electron is fixed, and the fluctuating field with the Larmor frequency of nuclei arises due to fast electronic relaxation. If the concentration of paramagnetic centers is small, then the time of transverse relaxation of electronic spins is large ($1/T_{2e} \approx \Delta\omega_{el}$ – ESR line width, or to be more precise, its homogeneous part) and then the fluctuating fields having some spectral density at NMR frequency are created by relaxation of longitudinal magnetization of electronic spins, i.e. S_z, and the time of spin-lattice relaxation of electrons T_{1e} serves as the correlation time. In the Hamiltonian of dipole-dipole interaction we are interested in the terms containing operators which can cause spin flip of nucleus, i.e. the terms, $\hat{C}$ and $\hat{D}$.

$$\hat{C} = -\frac{3}{2}\gamma_I \gamma_S \mathsf{h}^2 \cdot r^{-3} \sin\Theta \cdot \cos\Theta \cdot e^{i\varphi}(S_z I_+ + S_+ I_z),$$

$$\hat{D} = \hat{C}^*.$$

Here Θ – angle between the magnetic field direction and a radius vector connecting the nucleus and the electron. In both terms the second components are not necessary to us since they cannot cause nuclear transitions.

The calculations show that

$$\frac{1}{T_{1n}} = \gamma_I^2 \mathrm{h}^2 \int_{-\infty}^{\infty} < H_e(t) \cdot H_e(t-\tau) > \exp(-i\omega_I \tau) d\tau =$$

$$= \frac{9}{2} \gamma_S^2 \gamma_I^2 \mathrm{h}^2 \cdot r^{-6} \sin^2\Theta \cdot \cos^2\Theta \int_{-\infty}^{\infty} < S_z(0) S_z(\tau) > \exp(-i\omega_I \tau) d\tau;$$

$$< S_z(0) S_z(\tau) > = \frac{1}{3} S(S+1) \cdot \exp\left(-\frac{|\tau|}{T_{1e}}\right);$$

$$\mathrm{Re} \int_{-\infty}^{\infty} \exp\left(-\frac{|\tau|}{T_{1e}}\right) \cdot \exp(-i\omega_I \tau) d\tau = 2\,\mathrm{Re} \int_{-\infty}^{\infty} \exp\left(-\frac{|\tau|}{T_{1e}}\right) \cdot \exp(-i\omega_I \tau) d\tau =$$

$$= 2\,\mathrm{Re}\left(\frac{1}{1/T_{1e} + i\omega_I}\right) \cdot \int_0^{\infty} e^{-x} dx = -\mathrm{Re}\left(\frac{2T_{1e}}{1 + i\omega_I T_{1e}}\right) \cdot e^{-x} \Big|_0^{\infty} = -\mathrm{Re}\frac{2T_{1e}}{1 + i\omega_I T_{1e}} = \frac{2T_{1e}}{1 + \omega_I^2 T_{1e}^2};$$

$$\frac{1}{T_{1n}} = \gamma_S^2 \gamma_I^2 \mathrm{h}^2 \cdot r^{-6} \sin^2\Theta \cdot \cos^2\Theta \cdot S(S+1) \cdot \frac{T_{1e}}{1 + \omega_I^2 T_{1e}^2}.$$

More often the condition $\omega_I T_{1e} > 1$ is satisfied, therefore $\frac{T_{1e}}{1 + \omega_I^2 T_{1e}^2} = \frac{1}{\omega_I^2 T_{1e}}$.

Then, if we omit $\sin^2\Theta \cdot \cos^2\Theta$, i.e. the orientation dependence of T_{1n}, it is possible to write:

$$\frac{1}{T_{1n}} = \frac{\gamma_S^2 \mathrm{h}^2 \cdot S(S+1)}{r^6} \cdot \frac{\gamma_I^2}{\omega_I^2} \cdot \frac{1}{T_{1e}} = H_{loc}^2 \cdot \frac{\gamma_I^2}{\gamma_I^2 \cdot H_0^2} \cdot \frac{1}{T_{1e}} = \left(\frac{H_{loc}}{H_0}\right)^2 \cdot \frac{1}{T_{1e}},$$

where H_{loc} – a local field created by the electron spin on a nucleus.

$\frac{1}{T_{1e}} \sim \mathrm{cth}\left(\frac{\mathrm{h}\omega_e}{2kT}\right)$ for direct processes; at $T \to 0$ $\mathrm{cth}(...) \to 1$, i.e. the obtained result states that at low temperatures the nuclear relaxation rate via the paramagnetic impurities tends to a constant. The experiment shows that it is not the case: at

temperature lowering the nuclear relaxation rate decreases, approaching zero at $T \to 0$. This results from the fact that at low temperatures the electronic spins are essentially polarized. The account of polarization (relative difference of population of electronic energy levels) gives the additional factor in the equation for nuclear relaxation:

$$\frac{1}{T_{1n}} = 3\gamma_I^2 \gamma_S^2 \hbar^2 r^{-6} \cdot \sin^2\Theta \cdot \cos^2\Theta \cdot S(S+1) \cdot \frac{T_{1e}}{1+\omega_n^2 T_{1e}^2} \cdot (1 - P_0^2),$$

where $P_0 = \mathrm{th}\left(\hbar\omega_0 / 2kT\right)$.

3.2. Nuclear spin diffusion effect on nuclear relaxation via paramagnetic centers

Consider a chain of nuclei (I = 1/2) located at a distance a apart from each other (Fig. 8). We introduce p_+ – the probability that the spin is aligned "upwards", p_- – the probability that the spin is aligned "downwards"; then $p_+ + p_- = 1$, $p_+ - p_- = p$ – polarization.

The general problem is to find how polarization in this system changes and how the excitation propagates.

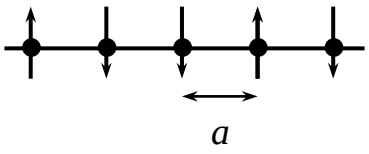

Fig. 8

The dipole-dipole interaction can induce the simultaneous flips of the two neighboring spins due to the term $B \sim I_{+i} I_{-j} + I_{-i} I_{+j}$, at that the Zeeman energy of the spin system is conserved (if the external field is much larger than the local field). How to find the probability of these mutual flips?

There is a local field $H_{loc} \sim \frac{\gamma\hbar}{r^3}(3\cos^2\Theta - 1) I_z$ on the given nuclear spin created by the neighbor. The probability of flip for the given spin in this local field is $W = \frac{\pi}{2}(\gamma H_{loc})^2 |< m_I \pm 1 | I_\pm | m_I >|^2$. But there is not only one neighbor at the given nucleus, every spin creates its local field which, besides, by causing the flips of the given spin, causes also a broadening of the NMR line. Hence, the local field has some distribution around zero and the probability of transitions shall also have a factor that

accounts for this distribution. Occurrence of this factor can be understood: if the spin that gives contribution to one wing of the NMR line flips, then this flip would hardly can cause flip of the spin that gives the contribution to the other wing of the NMR line since these two spins have different Zeeman energies, and at this transition the total Zeeman energy is not conserved. Hence, W will change as follows:

$$W = \frac{\pi}{2}(\gamma \bar{H}_{loc})^2 |< m_I \pm 1| I_{\pm} | m_I >|^2 \; g(\omega) = \frac{\pi}{2}(\gamma \bar{H}_{loc})^2 g(\omega) \text{ For } I = 1/2.$$

The line over $\bar{H}_{loc}$ means the average local field. $(\gamma \bar{H}_{loc})^2 = (\bar{\omega}_{loc})^2 = M_2$ - second moment of the NMR line. If broadening of the NMR line is homogeneous (caused only by dipole-dipole interactions), and nuclear spins form the regular lattice, then:

$g(\omega) = \frac{1}{\sqrt{2\pi M_2}} \exp\left[-\frac{(\omega - \omega_0)^2}{2M_2} \right]$, i.e. $g(\omega) = \frac{1}{\sqrt{2\pi M_2}}$ at resonance frequency.

Hence, $W \sim \sqrt{M_2}$ - half-width of NMR line. Exact calculations for a simple cubic lattice and a crystal crushed into powder give $W = \sqrt{M_2}/30$ for probability of mutual flips of pair of the neighboring spins.

Let's return to the linear chain of spins and try to write the kinetic equation for the polarization in a point with coordinate x (for one of spins):

$$\frac{\partial p_+(x)}{\partial t} = W p_-(x)[(p_+(x+a) + p_+(x-a)] - W p_+(x)[(p_-(x+a) + p_-(x-a)].$$

The first term reflects the fact that the probability for the given spin "up" is increased if at present the given spin is "down" and the neighbors are "up". The second term reflects the fact that the probability for the given spin "up" decreases if at present the given spin is "up" and the neighbors are "down". Here we deal with the conventional probability. It is necessary for two events to appear simultaneously and, hence, the equation includes the product of probabilities.

The spin in our model can be only in "up" or "down" positions, therefore

$$p_-(x) = 1 - p_+(x).$$

$$\frac{1}{W}\cdot\frac{\partial p_+(x)}{\partial t} = (1-p_+(x))[(p_+(x+a)+p_+(x-a)] -$$
$$-p_+(x)[(1-p_+(x+a)+1-p_+(x-a)] = p_+(x+a)+p_+(x-a)-2p_+(x).$$

In the same way $\frac{1}{W}\cdot\frac{\partial p_-(x)}{\partial t} = p_-(x+a)+p_-(x-a)-2p_-(x)$.

For the polarization we obtain:

$$\frac{1}{W}\cdot\frac{\partial p}{\partial t} = \frac{1}{W}\cdot\frac{\partial}{\partial t}(p_+ - p_-) =$$
$$=[p_+(x+a)-p_-(x+a)]+[p_+(x-a)-p_-(x-a)]-2[p_+(x)-p_-(x)],$$
$$\text{or}\quad \frac{1}{W}\cdot\frac{\partial p}{\partial t} = p(x+a)+p(x-a)-2p(x).$$

If we consider that polarization does not significantly changes from point to point,

$$p(x\pm a)\approx p(x)\pm\frac{\partial p}{\partial x}|_{x=0}\cdot a+\frac{1}{2}\frac{\partial^2 p}{\partial x^2}|_{x=0}\cdot a^2+\ldots$$

Then

$$\frac{1}{W}\cdot\frac{\partial p}{\partial t} = p(x)+\frac{\partial p}{\partial x}a+\frac{1}{2}\frac{\partial^2 p}{\partial x^2}a^2+p(x)-\frac{\partial p}{\partial x}a+\frac{1}{2}\frac{\partial^2 p}{\partial x^2}a^2-2p(x)=\frac{\partial^2 p}{\partial x^2}a^2,$$

$$\text{i.e.}\quad \frac{\partial p}{\partial t} = D\Delta p;\quad D = W\cdot a^2[\mathrm{s}^{-1}\cdot\mathrm{cm}^2];$$

$\Delta p = \frac{\partial^2 p}{\partial x^2}+\frac{\partial^2 p}{\partial y^2}+\frac{\partial^2 p}{\partial z^2}$ (generalization for the three-dimensional case).

The obtained equation is identical to diffusion equation: for diffusion there is a change of substance concentration through the surface area ΔS normal to change direction, the substance mass Δm is transferred per time $\Delta\tau$, proportional to a concentration gradient *dc/dx*, area ΔS, and time interval $\Delta\tau$,

$$\Delta m = -D\cdot\frac{dc}{dx}\cdot\Delta S\cdot\Delta\tau.$$

$$\text{Since}\ c=\frac{dm}{dV}=\frac{dm}{dx\cdot\Delta S},\ \text{then}\ \frac{\Delta m}{\Delta\tau}=-D\frac{dm}{dx}.$$

Let's estimate the order of magnitude for D. For example, we take ^{19}F (I = 1/2) nuclei in crystal CaF_2. The distance $r_{F–F}$ = 2.73 Å, the NMR line width for fluorine $\gamma \cdot 2.5\,\text{Oe} = 2\pi \cdot 4006\,\text{s}^{-1}/\text{Oe}$.

Hence, $\sqrt{M_2} = 2.5\,\text{Oe} \cdot \gamma = 6.3 \cdot 10^4\,\text{s}^{-1}$; $W = \sqrt{M_2}/30 = 2.1 \cdot 10^3\,\text{s}^{-1}$.

$D = W \cdot a^2 = 2.1 \cdot 10^3\ \text{s}^{-1} \cdot 7.5 \cdot 10^{-16}\ \text{cm}^2 = 1.6 \cdot 10^{-12}\ \text{cm}^2\text{s}^{-1}$. Usually $D \sim 10^{-13}\ \text{cm}^2 \cdot \text{s}^{-1}$.

Let's estimate the time for which the perturbation of polarization is transferred on the distance equal to half distance between paramagnetic centers (PC) at concentration of 0.1 %, i.e. on distance of the order of 30 … 40 Å. The mean-square length of diffusion polarization per time t is equal to $x^2_m = D\,t / 3$, hence $t \sim 0.5...5\,\text{s}$. It follows that the nuclei remote from the paramagnetic centers transfer their excitation to the nuclei that are close to the paramagnetic centers due to spin diffusion for 0.5 … 5 seconds, and those, in turn, transfer energy through the paramagnetic centers to a lattice.

In immediate proximity from PC the spin diffusion is difficult. Close to PC there is a local field which value at the distance r from PC is created and is equal to $H_{loc} \approx /\mu r^3$. If $\mu = \mu_B$, and r = 3 Å (as for the nearest to Er^{3+} protons in LaES:Er^{3+}, 0.1%), then H_{loc} = 343 Oe; at the distance of 6 Å, H_{loc} = 43 Oe; at the distance of 9 Å, H_{loc} = 13 Oe; at the distance of 12 Å, H_{loc} = 5 Oe.

If the proton NMR line width is 2 … 3 Oe, then the probability of flip-flop processes between the “normal” protons and the protons at which the field is different from normal on the value of local field created by paramagnetic center, will be very small if this field exceeds the NMR line width. This is evident from the equation for W:

$$W \sim \exp\left[-\left(\omega - \omega_0\right)^2 / 2M_2\right],$$

where $M_2 \approx \Delta^2$ – square NMR line width. If $\left|\omega - \omega_0\right| > \Delta$, then exp […] $\to$ 0.

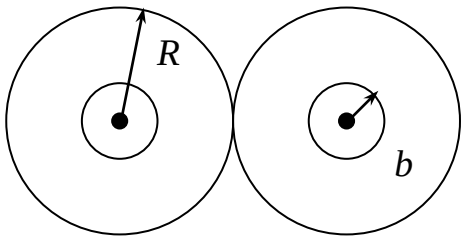

Fig. 9

Thus, the nuclear spin diffusion near the paramagnetic center is difficult. It is possible to determine the size of this area supposing that it is limited by some sphere with the radius *b* (see Fig. 9) on which surface the local field created by the paramagnetic center is equal to the NMR line width for the nuclei remote from the paramagnetic center, i.e. $\gamma_S \hbar / b^3 = \Delta H_n$. The radius *b* is called the radius of spin diffusion barrier. It is assumed that the uniform relaxation rate for all "normal" nuclei $1/T_{1n}$ is determined by averaging of the rates $1/T_{1n}(r)$ in a volume enclosed between the sphere with radius *b* and the sphere with radius approximately equal to half distance between the paramagnetic centers which is determined from the condition $V \cdot N_S = 1$, or $(4/3)\, R^3 \cdot N_S = 1$, where N_S – number of PC in the unit volume (in 1 cm^3):

$$\frac{1}{T_{1n}} = \frac{1}{V}\int_b^R \frac{1}{T_{1n}(r)} dV \approx \frac{8\pi}{5} \cdot \frac{N_S}{b^3} \cdot \frac{\gamma_S^2 \hbar^2}{H_0^2} \cdot \frac{S(S+1)}{3} \cdot \frac{1}{T_{1e}} \cdot (1 - P_0^2).$$

The equation can be rewritten in the other form if we remember that $\gamma_S \hbar / b^3 = \Delta H_n$, and on the other hand, ($\Delta H_n = \gamma_I \hbar / a^3$, *a* – distance between nuclei). $1/a^3 = N_I$ (really, N_I is equal to the number of nuclei in a cube with an edge of 1 cm. 1 cm is $1/a$ lattice constants, i.e. in 1 cm^3 there is $1/a^3$ unit cells (or the sites occupied with nuclei), i.e. $1/a^3$ nuclei). Thus $\Delta H_n \approx \gamma_I \hbar N_I$.

Using $\frac{1}{b^3} = \frac{\Delta H_n}{\gamma_S \hbar}$ and $\frac{\Delta H_n}{\gamma_I \hbar N_I} = 1$, we will rewrite the equation as follows:

$$\frac{1}{T_{1n}} \approx \frac{8\pi}{5} \cdot N_S \cdot \frac{\Delta H_n}{\gamma_S \mathrm{h}} \cdot \frac{\Delta H_n}{\gamma_I \mathrm{h} N_I} \cdot \frac{\gamma_S^2 \mathrm{h}^2}{H_0^2} \cdot \frac{S(S+1)}{3} \cdot \frac{1}{T_{1e}} \cdot (1 - P_0^2) =$$

$$= \frac{8\pi}{5} \cdot \frac{S(S+1)}{3} \cdot \frac{N_S}{N_I} \cdot \frac{\gamma_S}{\gamma_I} \cdot \left(\frac{\Delta H_n}{H_0} \right)^2 \cdot \frac{1}{T_{1e}} \cdot (1 - P_0^2).$$

$\frac{8\pi}{5} \cdot \frac{S(S+1)}{3} \sim 1$; $\frac{N_S}{N_I} \sim 10^{-2}...10^{-3}$; $\frac{\gamma_S}{\gamma_I} \sim 10^3$; $\left(\frac{\Delta H_n}{H_0} \right)^2 \sim 10^{-6}$; $\frac{1}{T_{1n}} \sim 10^{-5}...10^{-6} \frac{1}{T_{1e}}$.

The nuclear relaxation rate is much smaller than electron relaxation rate.

In reality the considered model underestimates slightly the possibilities of nuclear diffusion. Really, if the local field created by PC is increased "smoothly" when approaching to PC, i.e. if the local fields "sensed" by the two neighboring nuclei, differ less than NMR line width (though the local field itself can be stronger in comparison with the NMR line width), then the diffusion between them nevertheless is possible. In other words, the radius of diffusion barrier should be determined not from the rigid condition $\gamma_S \mathrm{h} / b^3 = \Delta H_n$, but from milder condition $a \frac{\partial}{\partial r} \left(\frac{\gamma_S \mathrm{h}}{r^3} \right)_{r=b} = \Delta H_n$, where a – lattice constant ($a \approx N_I^{-1/3}$). This approach reduces the radius of diffusion barrier and leads to $\left(\gamma_S / \gamma_I \right)^{1/4}$ times growth of T_{1n}^{-1} approximately compared with that obtained.

3.3. Nuclear relaxation via PC in the absence of nuclear spin diffusion

If the crystal contains enough the paramagnetic impurities it may happen that the radius of diffusion barrier becomes larger than half of average distance between the paramagnetic centers. In this case all nuclei appear in the area of difficult spin diffusion; i.e. there is no "normal" nuclei. The excitation cannot be transferred from a nucleus to a nucleus, each nucleus relaxes by itself through the nearest paramagnetic centers. Then there are two questions:

1. What impurity concentration approximately should be?

2. According to what law in this case the nuclear polarization after saturation changes, i.e. how the recovery curve of longitudinal magnetization looks like in this case?

The radius of diffusion barrier is $b^3 \sim \mu_e/\Delta H_n$; $\Delta H_n \sim \mu_n N_I$. The distance between the paramagnetic centers is $R^3 \sim 1/N_S$; $b^3 \sim R^3 \rightarrow \mu_e / (\mu_n N_I) \sim 1/N_S$; $N_S/N_I \sim \mu_n/\mu_e \sim 10^{-3}$, i.e. the diffusion becomes difficult if the concentration of the paramagnetic centers is ≥0.1 %.

The longitudinal magnetization recovery in "usual" case is $p\,(t) = 1 - M_t / M_\infty = \exp\,(-t/T_{1n})$. If each nucleus relaxes independently via the nearest paramagnetic center then the relaxation rate is different for different nuclei and then $p(t)$ may be written as follows:

$$p(t) = \exp\left[-t \cdot \sum_j \left(T_{1n}(r_{ij}) \right)^{-1} \right],$$

where summation is performed over all sites occupied by the paramagnetic centers. The equation can be written in the following form:

$$p(t) = \prod_j \exp\left(-\frac{t}{T_{1n}(r_{ij})} \right),$$

where j enumerates again the sites occupied by PC. It will be more convenient if j run over all sites of the lattice, both occupied and not occupied with the paramagnetic centers. If the relative concentration of PC is equal to c, then the probability to find the paramagnetic center by sorting all sites of the lattice is equal c, and the probability that a site is not occupied, is equal $1 - c$. Taking this into account it is possible to rewrite $p(t)$ as follows:

$$p(t) = \prod_j \left[c \cdot \exp\left(-\frac{t}{T_{1n}(r_{ij})} \right) + (1-c) \cdot 1 \right],$$

where j enumerates the lattice sites and the relaxation occurs if the given site is occupied by the paramagnetic center.

It is more convenient to rewrite the equation for $p\,(t)$ in the following form:

$$p(t) = \prod_j \left[1 - c\left(1 - \exp\left(-\frac{t}{T_{1n}(r_{ij})} \right) \right) \right].$$

If c is small (estimates have already shown that the diffusion is difficult when c is larger than 10^{-3}, but really it is not much), it is possible to rewrite 1- c (…) as the result of expansion of the exponent, i.e. $1 - c\,(\ldots) \approx \exp[-c\,(\ldots)]$, then

$$p(t) = \prod_j \exp\left[-c\left(1 - \exp\left(-\frac{t}{T_{1n}(r_{ij})} \right) \right) \right] = \exp\left[-c\sum_j \left(1 - \exp\left(-\frac{t}{T_{1n}(r)} \right) \right) \right] \approx$$

$$\approx \exp\left[-cN_I \int_V \left[1 - \exp\left(-\frac{t}{T_{1n}(r_{ij})} \right) \right] dV \right],$$

where N_I – total number of lattice sites (or $1/V$), $cN_I = N_S$ – number of sites occupied by PC, i.e. the absolute concentration of paramagnetic impurity.

If nuclei are coupled to paramagnetic centers by the dipole-dipole interaction,

$$1/T_{1n}(r) = A \cdot r^6 \cdot \sin^2\Theta \cdot \cos^2\Theta, \quad dV = r^2 \cdot \sin\Theta \cdot d\Theta \cdot d\varphi \cdot dr = r^2 \cdot dr \cdot d\Omega,$$

where $d\Omega$ – element of spatial angle. In this case

$$\int \left[1 - \exp\left(-\frac{t}{T_1(r)} \right) \right] dV = \int \left[1 - \exp\left(-A \cdot t \cdot r^6 \cdot f(\Omega) \right) \right] r^2 dr\, d\Omega,$$

where $f(\Omega) = \sin^2\Theta \cdot \cos^2\Theta$.

Let's designate $x = A \cdot t \cdot r^{-6} \cdot f(\Omega)$, then

$$r = (A \cdot t \cdot f)^{1/6} x^{-1/6};\; r^2 = (A \cdot t \cdot f)^{1/3} x^{-1/3}; dr = -\frac{1}{6}(A \cdot t \cdot f)^{1/6} x^{-7/6} dx.$$

Now we have

$$\int \left[1 - \exp\left(-t/T_1 \right) \right] dV = (A \cdot t)^{1/3} \left[-\frac{1}{6}(A \cdot t)^{1/6} \right] \times$$

$$\times \int \left[1 - \exp(-x) \right] x^{-1/3} \cdot x^{-7/6} \cdot f^{1/3} \cdot f^{1/6} \cdot dx \cdot d\Omega =$$

$$= -\frac{1}{6}(A \cdot t)^{1/2} \int \left[1 - \exp(-x) \right] x^{-3/2} dx \int f^{1/2}(\Omega) d\Omega\ .$$

Thus, in case of relaxation via the paramagnetic centers in the absence of nuclear spin diffusion we obtained that

$$p(t) = 1 - \frac{M(t)}{M(\infty)} = \exp\left(-\sqrt{\frac{t}{T_{1n}}}\right),$$

where

$$\frac{1}{T_{1n}} = \frac{4}{9} \cdot \pi^3 \cdot N_S^2 \cdot g^2 \cdot \mu_B^2 \cdot \gamma_I^2 \cdot \frac{\tau_c}{1 + \omega_I^2 \tau_c^2} \cdot (1 - P_0^2).$$

The obtained equation describes correctly the experiment if the paramagnetic impurities are distributed uniformly over the volume. Generally

$$p\,(t) \sim \exp\,[-\,(t/T_{1n})^{\,D/6}],$$

where D – dimensionality of distribution of the paramagnetic impurities. For flat lattice $D = 2$, for linear $D = 1$.

4. Methods of relaxation time measurements

One of the advantages of a pulsed method in comparison with continuous wave method is the possibility of direct measurements of the relaxation times – transverse (spin-spin) and longitudinal (spin-lattice) times. The transverse relaxation can be characterized by one parameter in the case when magnetization decay occurs exponentially. The NMR signal decreases in e times for time T_2. If there is the broadening of the line caused by heterogeneity of the applied magnetic field or distribution of internal local fields (so-called nonuniform broadening) then it is possible to estimate T_2 from the FID. In this case the transverse relaxation time is related to the NMR line width $\Delta\omega$ via the simple relation $T_2 = 1/\Delta\omega$. The nonuniform broadening accelerates decay of transverse magnetization and FID decreases with the time constant which can be designated as T_2^*. The spin echo method allows to measures the true value of T_2. The spin echo amplitude depends exponentially on time interval τ as shown in Fig. 10a. The simplest, though not the most exact

measuring method of the longitudinal magnetization time recovery, is the measurement of FID amplitude or echo depending on the pulse repetition period T. In this case the signal amplitude A depends on T as:

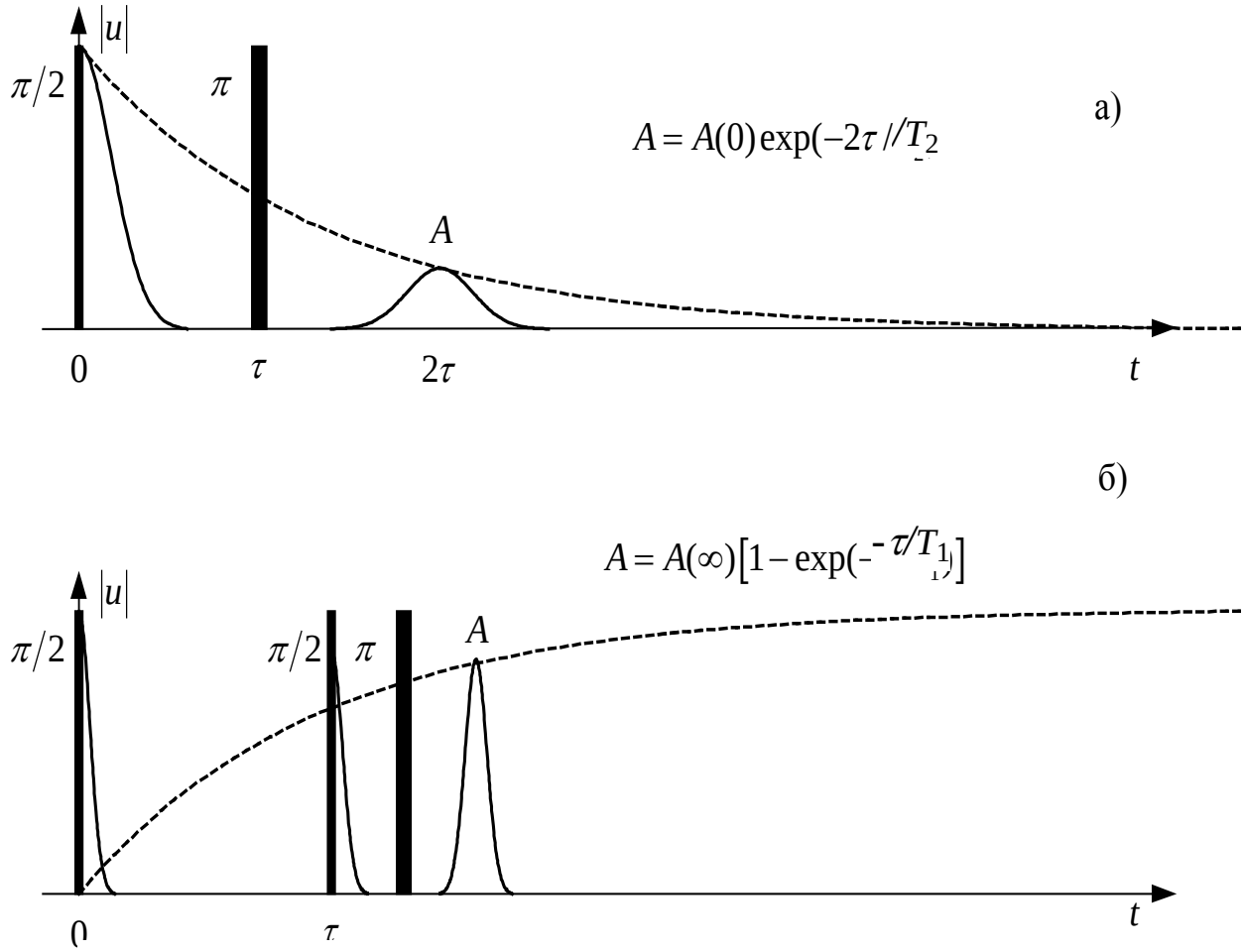

Fig. 10. a) Measuring technique of the transverse relaxation;
b) Measuring technique of the longitudinal relaxation.

$$A(\infty)\left[1-\exp(-T/T_1)\right].$$

The saturation – recovery method (Fig. 10b) is more popular. It is three-pulse sequence. The first $\pi/2$ pulse destroys the longitudinal magnetization (saturation). The second and the third $\pi/2$ and π pulses, respectively, are applied after time τ which form a spin echo signal.

The signal amplitude is proportional to the value of the longitudinal magnetization at the time τ. The time interval between the second and the third pulse remains invariable.

The repetition period of all pulse sequence should be not less than $5T_1$.

5. NMR pulsed spectrometer

5.1. Purpose

The pulsed coherent spectrometer is intended for recording the NMR signals and measurement of the spin-lattice and spin-spin relaxation times. The spectrometer receiver is of direct conversion with quadrature detection. The transmitter and receiver are broadband (5 … 50 MHz). The tunable circuits: probe and the quarter lambda network, that provides a quadrature of the reference voltages of synchronous detectors.

5.2. Technical characteristics

Frequency band	5 – 50 MHz
Probe:	
Operating frequency	13.740 MHz
Frequency band	330 kHz
Transmitter	
Input impedance	50 Ω
Video pulse input	TTL
Output impedance	50 Ω
Output power	25 W
Preamplifier of receiver	
Input and output impedance	50 Ω
Noise factor	1.5 dB

Gain	40 dB
Receiver	
Input impedance	50 Ω
Gain	60 dB
Band Width	100 kHz

5.3. Probe design

The inductance coil with the sample and the capacitor of the tank circuit are located in the gap between the poles of electromagnet (see Fig. 11).

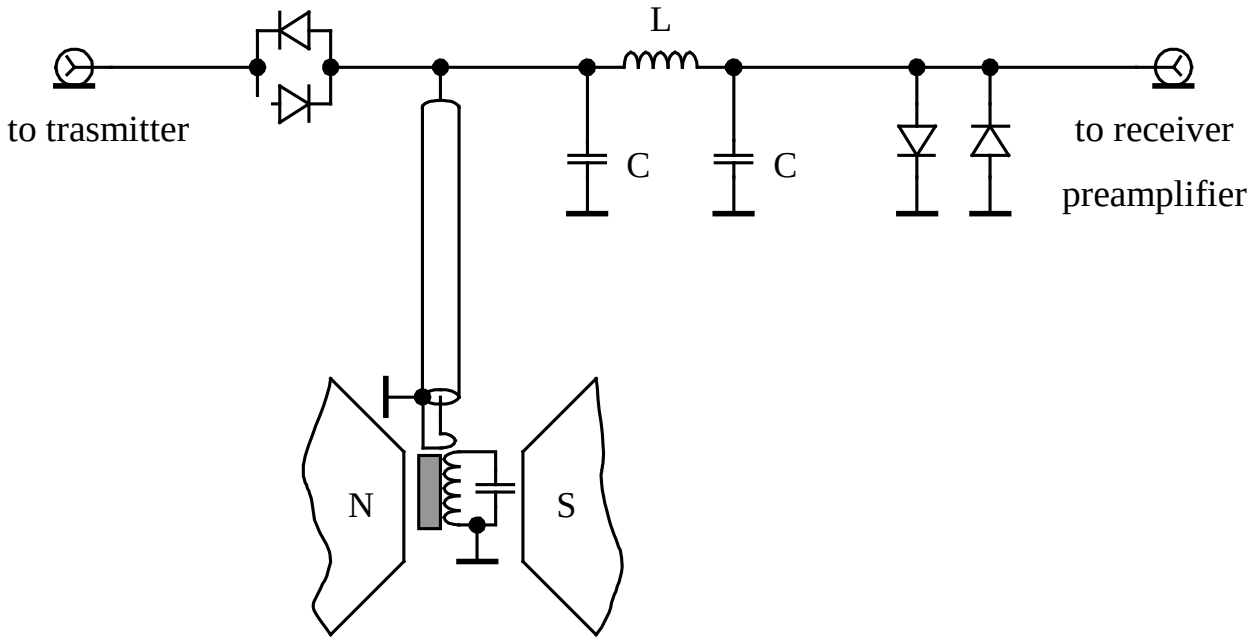

Fig. 11. Schematic diagram of the probe

With the help of inductive coupling the resistance of tank circuit at operation frequency is matched with the wave resistance of a coaxial cable, output resistance of the transmitter and the input resistance of the preamplifier of receiver – 50 Ω.

The probe construction allows to alternately commute alternately the oscillating circuit with transmitter and receiver. The transmitter is connected to the circuit at RF-pulses by means of the diode keys when the voltage on the transmitter output exceeds 1 V. For protection of the preamplifier of receiver at pulses the network equivalent to the quarter wave transformer is used. For a segment of line with length of quarter-

wave ($\lambda/4$) the relation $Z_0^2 = Z_1 Z_2$ relating the wave impedance of cable Z_0, load impedance Z_2 and the input impedance Z_1 is valid. The quarter wave circuit is equivalent to this segment if its inductance and capacitance satisfy the relations $Z_0 = \sqrt{L/C}$, $\omega = 1/\sqrt{LC}$, where Z_0 – wave impedance of the equivalent segment of the line, and ω – operational frequency of a spectrometer. During the pulse the diodes on the output of $\lambda/4$ chain are conducting, Z_2 is small, and therefore Z_1 is much larger than 50 Ω. The output power of the transmitter completely enters into the circuit, and the high voltage at the preamplifier input is absent. In the absence of pulses the transmitter is disconnected, and tank circuit is in matched junction with the preamplifier input.

5.4. Operation principle

The functional assemblies and voltage waveforms in different points of a spectrometer are presented on the block-diagram (Fig. 12). The harmonic oscillations on a synthesizer output are modulated in the RF pulse-former by video pulses from the generator Г5-82 output. Radiofrequency pulses are amplified and feed on the probe. The NMR signal is amplified by the portable low-noise preamplifier, then by the amplifier of the receiver and feed on the input of the quadrature detector. The latter corresponds to the two analogue multipliers of voltages and the low-pass filter (LPF) at which the phases of reference voltages are shifted on $\pi/2$ relative each other, i.e. are in a quadrature. The quadrature detector relays the signal spectrum to low-frequency region on the value ω, where ω – frequency of the frequency synthesizer, and allows to distinguish the frequencies above and below the latter. LPF eliminates the combination frequencies of the order of 2ω which are formed due to multiplication. The output signals of the quadripole detector are proportional to values of M_x and M_y of RF rotating with a frequency ω with the corresponding choice of the reference signal phase. The two output signals of the receiver can be considered also as the complex signal which Fourier-transformation gives a spectrum with zero frequency corresponding to the frequency ω of a spectrometer.

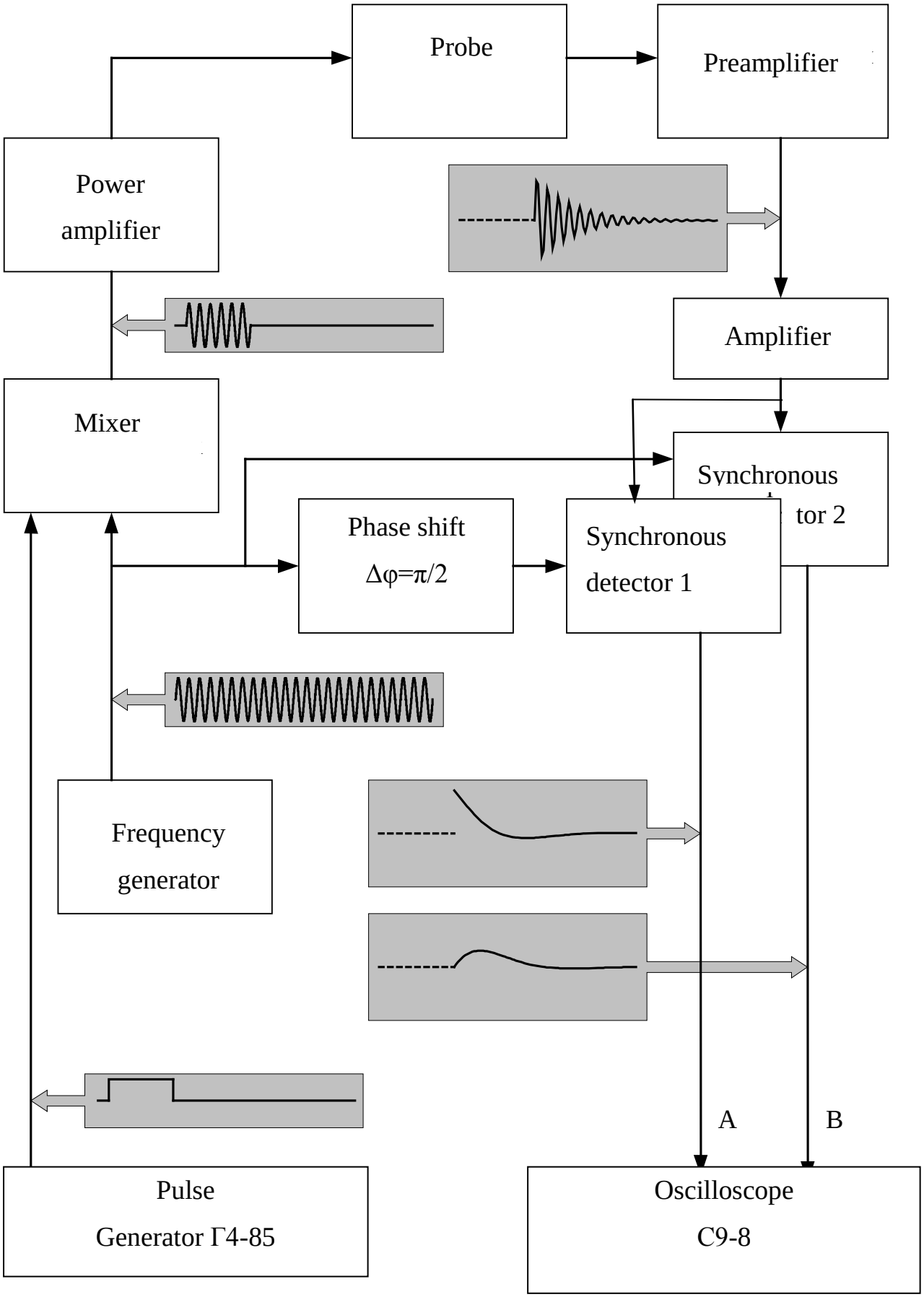

Fig. 12 Block diagram of a pulse spectrometer.

6. Recording and processing of the pulse NMR signals

Recording and processing of NMR spectra is carried out with the digital oscilloscope АСК-2167 and computer with the help of the corresponding software.

First of all, it is necessary to prepare the oscilloscope for operation and obtain the image of complex NMR signal on its screen. Then, having established the connection between the computer and oscilloscope to carry out data transmission and its display on the computer.

6.1. Preparation of oscilloscope for operation and observation of NMR signals

For preparation of oscilloscope for operation it is necessary to perform the following settings.

a) Perform the automatic calibration of the device. For this purpose it is necessary to disconnect all cables from the input sockets. Open the SYSTEM menu by the button UTILITY, press the button F3 (autocalibration), then – F2 (factory settings). Select language by the button F4 (for example, Russian or English).

b) Set the channels of vertical scan CH1 and CH2. Open the menu of the channel with the corresponding button CH MENU and set the following:

input – DC,

channel – on,

tester – 1×,

invert. – off.

c) Select the elements of timing control. Call the menu by TRIG MENU and set the following:

type – single,

source – external,

type – front,

front – decay,

triggering mode – standby,

input – DC.

d) Prepare the oscilloscope for measurements. Open the menu by MEASURE button and set the measured quantity:

source – type

channel 1 – V_{max},

channel 1 – V_{min},

channel 2 – V_{max},

channel 2 – V_{min},

and, by opening the corresponding menu by the button CURSOR set the following:

type – voltage,

source – channel 1 (or channel 2).

For both channels

cursor 1 – 0.0 mV,

cursor 2 – 0.0 mV,

difference – 0.0 mV.

By handles VOLT/DIV set the division value of the vertical scale (for example, 5V). All these settings will be necessary also for measurements of the relaxation time with this oscilloscope.

For observation of the NMR complex signal form on the oscilloscope screen it is necessary to apply the output quadrature signal of the NMR spectrometer receiver on the inputs of oscilloscope channels CH1 and CH2, in our case – the signal of spin induction (SSI) in some orientation of the sample relative the magnetic field (for example, **H** || [111]).

Arrange the signals of channels CH1 and CH2 on the screen in the opposite sides from the central horizontal line and match zero levels of signals with it. Perform fine-tuning of the magnetic field from the signal appearance on the oscilloscope screen: the beginning of the registered signal decay of one channel shall concur with the beginning of the registered signal decay of the other channel.

Match the beginning of the registered free induction decay (FID) with central vertical line on the oscilloscope screen by the horizontal position adjusting knob POSITION. The so-called “dead time” of the receiver t_{MB} for this orientation of the sample is determined as

$$t_{MB} = t_{\max} - \tau,$$

$t_{\max}$ – time, corresponding to a maximum of the observed SSI on the screen, τ – duration of the probing radio-pulse.

The voltage value in any point of the pulse can be measured with the help of the horizontal cursors directly on the oscilloscope screen.

6.2. Start of data transmission and mapping to the computer. Data saving and processing

Perform fine-tuning of the magnetic field from the signal appearance on the oscilloscope screen and engage the NMR-stabilization. Further action and settings are as follows.

1. Connect the oscilloscope with the computer by the USB cable.
2. Start the Oscilloscope program.
3. Establish connection between the computer and the oscilloscope.

a) Select successively the menu items

Communication → Port Setting.

In the appeared window check the setting **Connect using → USB** and the presence of information about the oscilloscope **Available port**.

In case of its absence close the program, disconnect the USB cable and repeat connection.

b) Select successively the menu items:

Communication → Continue data download (USB and Serial Port supported),

thereby starting the data transmission and mapping from the oscilloscope on the computer.

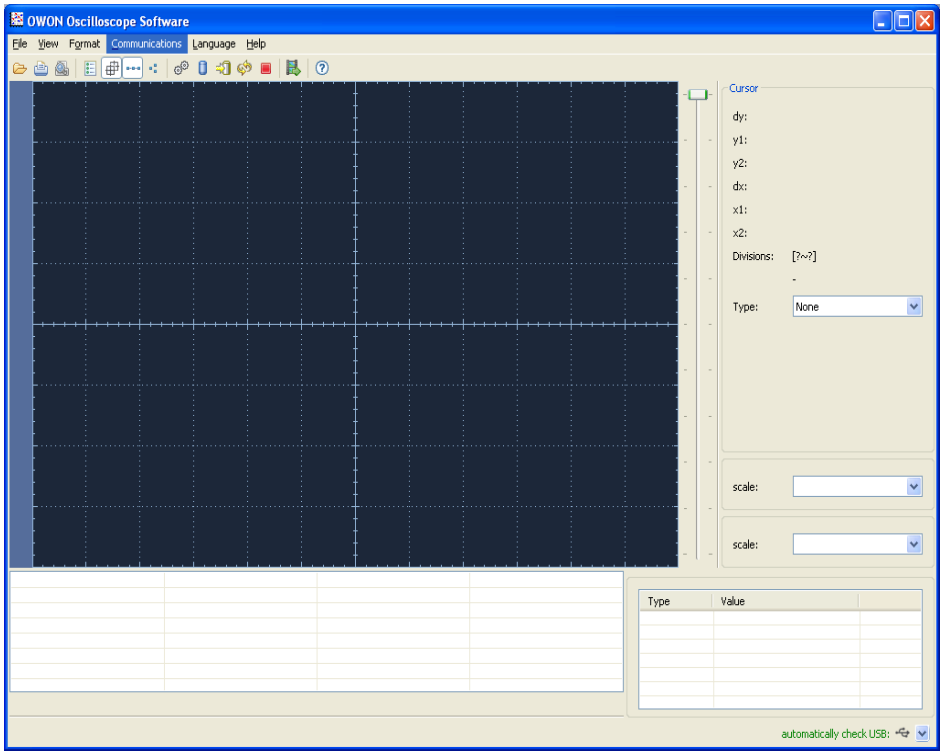

Fig. 13. The program for work with the oscilloscope.

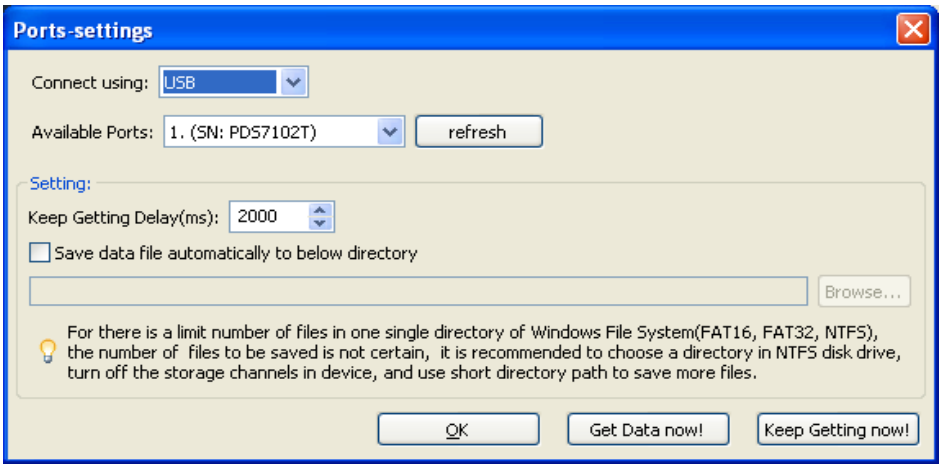

Fig. 14. USB Port settings.

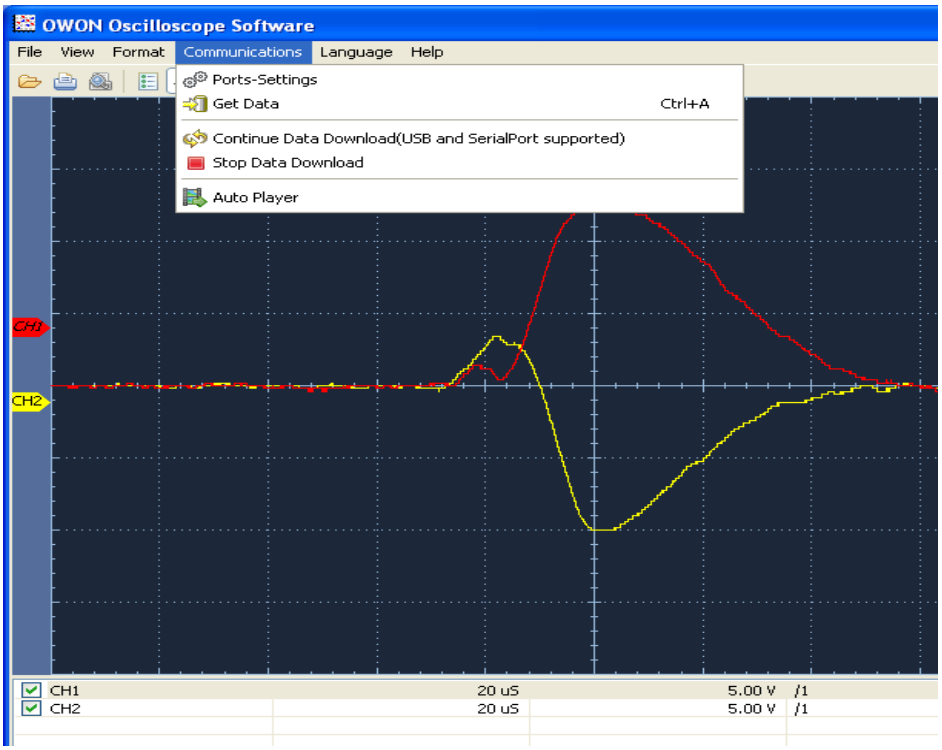

Fig. 15. Start of the data transmission and mapping.

4. To save the data from the oscilloscope to a file it is necessary to successively choose the menu items **View → Data table**, by opening a window shown in Fig. 16.

To save the data it is necessary to press the button SAVE AS.

In the appeared window for file selection (Fig. 17) it is necessary to create a folder with the number of your group in C:\TMP\ (it is created once at the first saving). Then to enter a file name (do not forget to specify in it the current crystal orientation) and type of the data. For further work in program Origin 7.0 (or the earlier version) it is recommended to save the data in the ASCII format - **Comma separated value text (*.csv)**. For older versions of Origin it is possible to save the data in **Microsoft Excel - Excel (*.xls)** format. For other software packages (Matlab, MatCad, etc.) it is necessary to specify first a format of the input data of this package.

In the saved file the first column corresponds to the point number. Therefore these digits at Fast-Fourier-Transformation shall be recalculated in the time values. For this purpose it is necessary to remember the values of scanning speed of oscilloscope *Td* (usually 20 μs per division, with 10 divisions in all scale). Further it is necessary to determine the number of points *N* in the saved spectrum.

Then the values of the first column shall be recalculated using the following equation:

$$t_i = i\,\frac{10 \cdot Td}{N},$$

where i –point number, t_i – value of this point on a time scale.

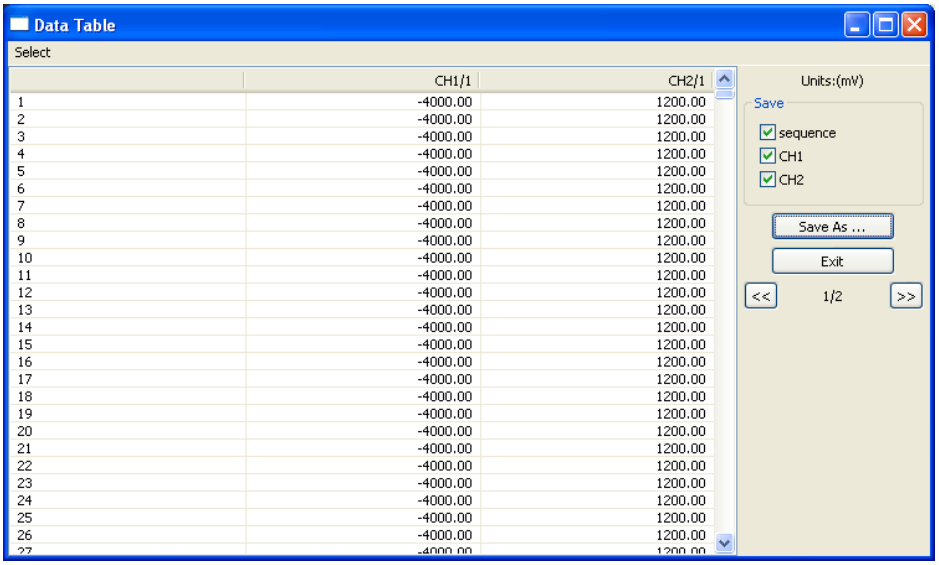

Fig. 16. Data table.

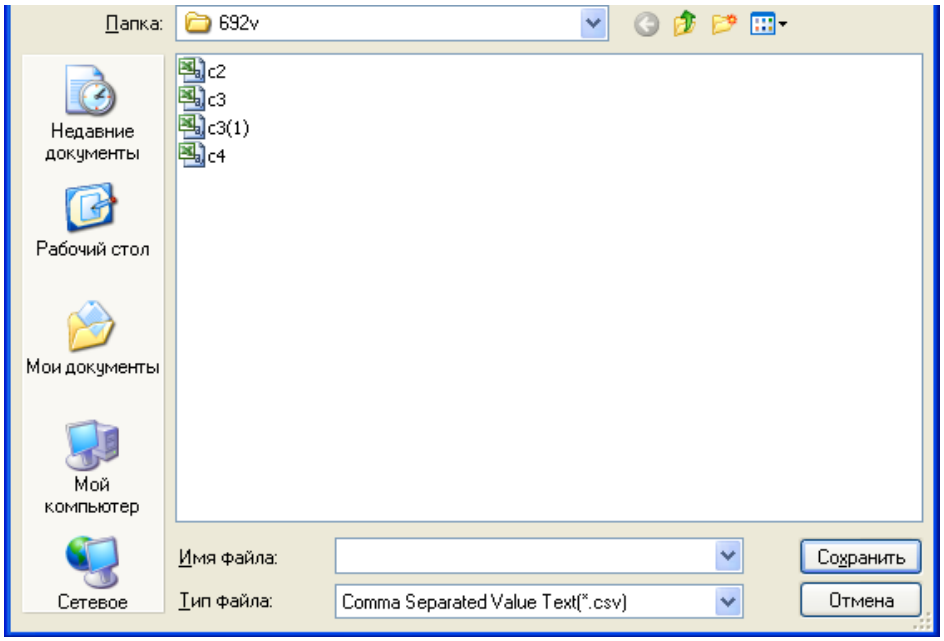

Fig. 17. File saving window.

6.3. Spin-lattice relaxation time measurement by the SSI signal saturation method

When measuring by this method it is necessary to determine the time for which the NMR signal intensity U will decay in e times when decreasing the pulse period T (item 3.3).

Switch on the current image on the oscilloscope screen. If necessary tune the magnetic field and obtain the correct image of a curve on the screen, then engage the NMR-stabilization of the magnetic field.

Select a reference voltage phase of quadrature detector of the receiver so that the one of the total signal components is equal to zero. Then the second component will be the total signal. The measurements shall be carried out at some point M of this component.

Check up the presence of the one of horizontal cursors on the central horizontal line of the oscilloscope screen (there shall be also zero levels of the signals of both channels). Match the second horizontal cursor with point M on the signal image. Record the corresponding T values (in ms) and U (difference of cursor indications in V) in the table and plot the change of signal intensity versus the pulse repetition period. Estimate the spin-lattice relaxation time using the equation

$$A = A(\infty)\left[1 - \exp(-T / T_1)\right].$$

Task

1. Set the parameters of the radio-frequency pulses of the transmitter on the pulse generator –

pulse repetition T = 1 s,

pulse duration τ = 3.1 μs,

pulse amplitude A = 5 V,

triggering – internal, single pulses,

on frequency synthesizer –

typeset the number– 6869, then the frequency value at the output **f/2** will be determined from the equation $\nu = (6869 \cdot 4 + 4)/2$.

Tune the field for resonance, activate the NMR-stabilization. Estimate the duration of a $\pi/2$ pulse (the signal amplitude is equal to zero for a π pulse).

2. Record the form of the complex NMR signal by points in orientations [100], [110] and [111].

3. Measure the spin-lattice relaxation time in three orientations, changing the pulse repetition period from 1 second to 10 milliseconds.

Additional task:

Compare the shape of signals with inverse Fourier transform of stationary NMR signal (Laboratory practical work “Continuous wave nuclear magnetic resonance”).

References

1. A. Abragam, The principles of nuclear magnetism. Oxford: Clarendon Press, 1961.
2. C. P. Slichter, Principles of magnetic resonance // Springer Series in Solid State Sciences, Springer-Verlag – 2nd edition, 1980.